NASA CR-134764

FABRICATION AND EVALUATION OF POLYMERIC EARLY-WARNING FIRE-ALARM DEVICES

by

Stephen D. Senturia

Department of Electrical Engineering and Computer Science
Massachusetts Institute of Technology
Cambridge, Massachusetts

prepared for

NATIONAL AERONAUTICS AND SPACE ADMINISTRATION

NASA Lewis Research Center

Contract NAS 3-17534

R.E. Gluyas, PROJECT MANAGER

1. Report No.	2. Government Accession No.	3. Recipient's Catalog No.
NASA CR-134764		

4. Title and Subtitle	5. Report Date
FABRICATION AND EVALUATION OF POLYMERIC EARLY-WARNING FIRE-ALARM DEVICES	6. Performing Organization Code

7. Author(s)	8. Performing Organization Report No.
Stephen D. Senturia	10. Work Unit No.

9. Performing Organization Name and Address	11. Contract or Grant No.
Massachusetts Insitute of Technology 77 Massachusetts Avenue Cambridge, Massachusetts 02139	NAS 3-17534

12. Sponsoring Agency Name and Address	13. Type of Report and Period Covered
National Aeronautics and Space Administration Washington, D.C. 20546	Contractor Report
	14. Sponsoring Agency Code

15. Supplementary Notes

NASA Project Manager, Richard E. Gluyas, Materials and Structures Division, NASA Lewis Research Center, Cleveland, Ohio

16. Abstract

The objective of this program is the exploitation of the fact that the electrical resistivities of some polymers are known to be enhanced by the presence of certain gases, in order to make a device capable of providing early warning to fire through its response with the gases produced in the early phases of combustion. Eight polymers were investigated: poly(phenylacetylene), poly(p-aminophenylacetylene), poly(p-nitrophenylacetylene), poly(p-formamidophenylacetylene), poly-(ethynyl ferrocene), poly(ethynyl carborane), poly(ethynyl pyridine), and the polymer made from 1,2,3,6 tetramethylpyridazine. A total of 40 usable thin-film sandwich devices and a total of 70 usable interdigitated-electrode "lock-and-key" devices were fabricated. The sandwich devices were used for measurements of contact linearity, polymer conductivity, and polymer dielectric constant. The lock-and-key devices were used to determine the response of the polymers to a spectrum of gases that included ammonia, carbon monoxide, carbon dioxide, sulfur dioxide, ethylene, acrolein, water vapor, and normal laboratory air. Strongest responses were to water vapor, ammonia, and acrolein, and depending on the polymer, weaker responses to carbon dioxide, sulfur dioxide and carbon monoxide

(continued)

17. Key Words (Suggested by Author(s))	18. Distribution Statement
fire-alarm devices polymers gas detection	UNCLASSIFIED-UNLIMITED

19. Security Classif. (of this report)	20. Security Classif. (of this page)
UNCLASSIFIED	UNCLASSIFIED

For sale by the National Technical Information Service, Springfield, Virginia 22151

were observed. A fire test was designed to determine the responses of devices to the emanations of a standardized smouldering fire. Six of the eight polymers showed usable responses to the test fires, and merit more detailed study for this application. Devices recovered after each test and multiple tests of individual devices showed good repeatability. A set of forty devices made from poly(p-aminophenylacetylene) were exposed to test environments for one month to determine the effects of aging and exposure to office, home, and outdoor conditions. Average device performance degraded somewhat after exposure, but most devices did respond to the test fire after exposure. Analysis of the gas-test and fire-test data indicate the presence of both bulk and surface effects in the response of the lock-and-key devices. A quantitative theory of device operation, capable of accounting for observed device leakage current and sensitivity, was developed. A prototype detection/-alarm system was designed and built for use in demonstrating sensor performance. Areas for constructive future work include: humidity compensation of individual devices, use of multiple-polymer devices for improved specificity of response, and device miniaturization for greater sensitivity.

TABLE OF CONTENTS

LIST OF FIGURES

LIST OF TABLES

PART I

INTRODUCTION AND SUMMARY

CHAPTER 1 Background of the Program

This program is the outgrowth of an earlier NASA sponsored program to develop "Space Cabin Atmosphere Contaminant Detection Techniques" (Contract NAS 12-15).[1] The objective of that program was to use polymers for gas detection, relying on the fact that the electrical conductivity of some polymers are known to be enhanced by the presence of certain gases. This may be the result of complex formation and transfer of charge between the gas molecule and the polymer. Other alternate explanations for the conductivity enhancement have been proposed, but the influence of gases on the conductivity of polymers is well established and has been well documented in the literature.[2]

The principal results of the earlier program can be summarized as follows: Four polymers were investigated, including poly(phenylacetylene) and three of its derivatives.[i.e., poly(p-nitrophenylacetylene) poly-(p-aminophenylacetylene), and poly(p-formamidophenylacetylene)]. These polymers could be formed into films, which made them suitable for device use. A series of tests were made on the sensitivity to ammonia gas of a device consisting of an interdigitated electrode structure (the "lock-and-key") coated with a thin film of poly(p-nitrophenylacetylene). Device conductance was observed to increase by one to three orders of magnitude on exposure to ammonia gas. Tests were also made on the degree of specificity of response of each of the four polymers. All polymers

showed a marked response to water vapor, while the different polymers responded differently to other gases. Finally, a portable prototype gas detector was fabricated using a two-sensor method. One device was coated with poly(p-nitrophenylacetylene), the other with poly(p-aminophenylacetylene). The sensors were connected to a circuit that measured any unbalance in the conductances of the two devices. Because of the differing responses of the two sensors to various gases, it was possible to detect SO_2 in the 10 ppm range (with the amino polymer responding more than the nitro polymer) and NH_3 in the 5 ppm range (with the nitro polymer responding more than the amino polymer). It is important to note that although both sensors responded more strongly to water vapor than to either of the gases being sensed, it was possible by using a combination of two sensors and an appropriately designed detection circuit to detect small changes in the concentration of the appropriate gas in a normal laboratory ambient. This result is of great significance in the ultimate design of a early-warning fire-alarm device.

The realization that the results described above might have application to the fire-detection problem occurred during the Urban Development Applications Project (UDAP) carried out by Abt Associates Inc. for the NASA Technology Utilization Division (Contract NASw-2022).[3] The UDAP program had two broad objectives: (1) to promote the application of aerospace technology to urban problems, and (2) to develop effective and efficient methodologies for transferring technology from its original aerospace context to the context of marketable products applicable to the

needs of urban society. Specifically, the UDAP program emphasized the identification of key problem areas, the identification, where possible, of NASA-developed technology that had the potential of making a unique contribution toward solving some aspect of an identified problem, and the development of modes of program management which would aid the transfer of the appropriate NASA developed technology to its new context.

One problem area identified in the UDAP program was the need for a low-cost, reliable, early-warning fire-alarm device. The work reported in reference 1 was identified as applicable to the fire-alarm problem from a literature search of the NASA data base. Two of the investigators on the present contract (Senturia and Colton) participated in this aspect of the UDAP program as members of a team of MIT faculty members who provided technical support for the UDAP effort. The UDAP team concluded that polymer detectors represented the most promising new technology for fire-alarm device application then in the NASA data base, and recommended in late 1971 that NASA Technology Utilization Division undertake a program of developmental engineering to promote the transfer of this technology.

During the period 1971-73, a group at MIT led by Senturia began a systematic investigation of device structures that would be appropriate to polymer-based fire-alarm devices, and on specific physical properties of some of the polymers. Two thesis projects[4,5] were initiated, on internal MIT funds, to explore this new field. The results of these research projects included several novel device concepts for potential use in the NASA program.

In mid-1973, two contracts were initiated by NASA Technology Utilization through the NASA Lewis Research Center. One of these (Contract NAS 3-17515 awarded to McDonnell Douglas Corporation[6]) called for the development of new polymeric materials; the other (Contract NAS 3-17534, awarded to MIT) called for the fabrication and evaluation of actual devices using polymers supplied by McDonnell Douglas. This report is the Final Contract Report for the MIT program.

CHAPTER 2 CONTRACT ACTIVITY

This contract called for a set of specific tasks that can be summarized as follows:

1. Device design and fabrication: The development of prototype devices and their fabrication using polymeric materials supplied by NASA.
2. Electrical measurements: Determination of basic electrical parameters that characterize the polymeric materials (conductivity, dielectric constant, contact properties).
3. Response to gases: Determination of the response of various polymers to a spectrum of pure gases, individually and in the presence of normal ambient air.
4. Fire tests: Determination of the response of various polymers to a standard cellulosic fire.
5. Long-term tests: Determination of the reproducibility and aging characteristics of devices, including possible effects of contaminants present in normal ambients, and effects of exposure to temperature variations and to light.
6. Deliverable items: Design and construction of a complete detection alarm system including five devices, for delivery to NASA, incorporating the best available polymer and device configuration.

CHAPTER 3 SUMMARY OF RESULTS AND RECOMMENDATIONS

A. Results

The principal results of this contract can be summarized as follows (details and supporting discussions are contained in Part II of this report):

1. Device design and fabrication: A total of 40 usable thin-film sandwich devices were fabricated using four of the eight NASA-supplied polymers. A total of 70 usable lock-and-key devices were fabricated using all eight NASA-supplied polymers. These devices were used in the various tests described below. In was concluded that device configurations in which the polymer application is the final step are to be preferred to configurations for which device processing is required after polymer application. This finding has implications for the types of miniaturized field-effect devices one can hope to manufacture (see section B.5 below).

2. Electrical measurements: Thin-film sandwich devices were used for measurements of contact linearity, polymer conductivity, and polymer dielectric constant.

3. Response to gases: Lock-and-key devices were used to determine the response of all NASA supplied polymers to a spectrum of gases that included ammonia, carbon monoxide, carbon dioxide, sulfur dioxide, ethylene, acrolein, water vapor, and normal laboratory air. Strongest responses were to water vapor, ammonia, and acrolein, and depending on the polymer, weaker responses to carbon dioxide, sulfur dioxide and carbon monoxide were observed. No response to ethylene was observed.

4. Fire Tests: A fire test was designed, using a small cotton charge (6 mg) heated to smouldering and using an air-flow system so that air of various relative humidities could be passed through the device chamber. Parameters of air flow, size of cotton charge, and heater power were standardized to achieve reproducible tests on lock-and-key devices coated with poly(p-aminophenylacetylene). Subsequent tests on all polymers showed that of the first four polymers supplied by NASA (these being poly-(phenylacetylene), poly(p-aminophenylacetylene), poly(p-nitrophenylacetylene), and poly(p-formamidophenylacetylene)), the amino polymer responded most strongly to the standard fire. Of the second four polymers supplied by NASA, the polymer made from 1,2,3,6 tetramethylpyridazine and the poly-(ethynyl pryidine) showed good responses and warrant further study. The formamido polymer and poly(ethynyl ferrocene) also showed good responses. The effect of humidity on the fire response is to shift the baseline device conductance (in the absence of the fire) but not the ratio of the peak conductance (in the presence of fire) to the baseline conductance. This means that if the baseline variation with humidity can be compensated (see section B.2) below), the devices will work effectively in a wide range of ambient humidities

5. Long-term tests: Poly(p-aminophenylacetylene) was selected for long-term tests as the best polymer then available. A set of 40 lock-and-key device substrates were made, from which a set of 25 were selected and coated. Ten of the devices were coated from 10% solutions, the remaining from 4% solutions. Before exposure to various environments,

the 10% devices responded significantly better to the standard fire than did the 4% devices. Since the 10% devices have a thicker polymer film than the 4% devices,this result demonstrates the presence of a bulk polymer response. Devices were placed in varied environments for one month (a kitchen, an office, a refrigerator, a nitrogen dry box, and out of doors). The characteristics of the 4% devices were varied and unpredictable after exposure. The 10% devices still responded uniformly after exposure, although with some loss of sensitivity.

6. Deliverable items: A set of devices was selected for delivery to NASA, and a detection/alarm system was designed and built for the purpose of demonstrating sensor performance.

7. Device theory: A quantitative theory of device operation was developed, and applied to the results obtained with lock-and-key devices. The theory is capable of accounting quantitatively for observed device leakage current (which in turn places a lower limit on device sensitivity) and predicts that better device performance will be achieved in present device geometries with polymers that have in vacuuo conductivities of 10^{-12} $(ohm-cm)^{-1}$, or, if using present polymers (which have lower conductivities), by miniaturizing the device geometry.

B. Conclusions and Recommendations

Based on the results as summarized above, it is concluded that:

1. Feasibility: The use of polymers to detect the emanations of incipient smouldering fires is feasible.

2. Discrimination and humidity compensation: Each polymer responds to a variety of gases, but to differing degrees. Therefore, added discrimination against unwanted responses, such as to humidity changes, can be achieved by combining several polymers into one alarm device. An example of such a combination-of-polymers approach would be the incorporation of carbon-impregnated cellulose into a device. This material is presently used for humidity detection in meteorological instrumentation.

3. Existing polymers: Several of the polymers studied in this program are promising fire-detection materials. Additional work on these polymers is needed to determine (a) which components of the emanations from the incipient fire are actually being detected by these polymers, and (b) what combination of polymers will yield optimum fire-detection sensitivity under expected normal ambients.

4. New polymers: Device sensitivity will be enhanced if new materials can be found which have higher in vacuuo conductivities (on the order of 10^{-12} $(ohm\text{-}cm)^{-1}$) but which have sensitivities (percent change in conductivity on exposure to gas) comparable to existing polymers.

5. Device miniaturization: Improved device sensitivity can be achieved by device miniaturization. A device concept developed at MIT (reference 4) is recommended as the soundest approach toward achieving an inexpensive and easy-to-manufacture device that will be compatible with silicon microcircuit technology.

PART II

TECHNICAL REPORT

CHAPTER 4 DEVICE FABRICATION

4.1 Polymers

A total of eight polymers were supplied by NASA. Table I shows a list of these polymers, a set of abbreviated names to be used throughout this report, and a summary of the types of devices successfully made from each polymer and the types of tests performed.

All polymers were received as powders (except for PEC, which was in a congealed form). Solutions in the appropriate solvent were made by thorough stirring followed by filtering. Concentrations of 4%, 5%, 10% and 20% were used at various times; however, the majority of solutions were 4%.

Polymer films were produced on substrate by spin coating, a standard technique for applying photoresist to silicon wafers. The substrate (glass microscope slide) was placed in a horizontal position on a chuck and held with a slight vacuum. The solution was placed on the slide. The slide was then spun in a horizontal plane for a brief period. Variations of spinning rate and spinning time were tried. At the slower speeds (below 4000 rpm), excess solution would not be thrown off of the slide, leaving a ridge of excess material at the edges of the device. At the higher speeds (above about 8000 rpm), the films showed signs of tearing. Best

TABLE I

SUMMARY OF POLYMERS, DEVICES AND TESTS

POLYMERS			DEVICE TYPE		TESTS PERFORMED					
POLYMER NAME	ABBREVIATION	SOLVENT	SANDWICH DEVICES	LOCK-AND-KEY DEVICES	CAPACITANCE	CONDUCTANCE	PATTERNING TEST	GAS TESTS	FIRE TESTS	LONG TERM
poly(phenylacetylene)	PPA	Benzene	x	x	x	x	x	x	x	–
poly(p-aminophenylacetylene)	PAPA	Dimethyl formamide	x	x	x	x	x	x	x	x
poly(p-nitrophenylacetylene)	PNPA	Acetone	x	x	x	x	x	x	x	–
poly(p-formamidophenylacetylene)	PFPA	Dimethyl formamide	x	x	x	–	x	x	x	–
poly(ethynyl ferrocene)	PEF	Benzene	–	x	–	–	x	x	x	–
poly(ethynyl pyridine)	PEP	Glacial acetic acid	–	x	–	–	–	x	x	–
poly(ethynyl carborane)	PEC	Methyl alcohol	–	x	–	–	–	x	x	–
polymer from 1,2,3,6 tetramethylpyridazine	PTMP	Glacial acetic acid	–	x	–	–	–	x	x	–

results were obtained at spinning speeds of about 6000 rpm. A spinning time of 15 seconds was used for most devices. No marked effects of varying this time were noted.

Films of PPA were examined under a polarizing microscope for evidence of optical anisotropy that might be produced by the spinning process. None was observed.

Film thickness of films of the amino polymer (PAPA) were measured using a scanning electron microscope. Slides coated with polymer were fractured,and examined along the fractured edge. Figure 1 shows a photomicrograph of the edge of a PAPA film spun from a 20% solution, viewed with 13,500 magnification. The measured film thickness is 3.6 microns. A scan of the fractured edge revealed that the film is remarkably uniform, with thickness variation estimated at 5% or less. A second film, spun from a 4% solution, was measured using the same technique, and was found to have a thickness of 0.9 microns, There is, thus, a monotonic dependence between film thickness and solution concentration. It has not been determined whether this dependence is a linear one; nor has the corresponding dependence been measured for other polymers.

The quality of the spun films was very dependent on the cleanliness of the solution. At various times during the project, films of poor quality were obtained using the same techniques that had yielded good films previously. Examination of the films under a microscope showed that the films were crystallizing, and that crystallization seemed to be associated with specks of dust or of what may have been cross-linked polymer within

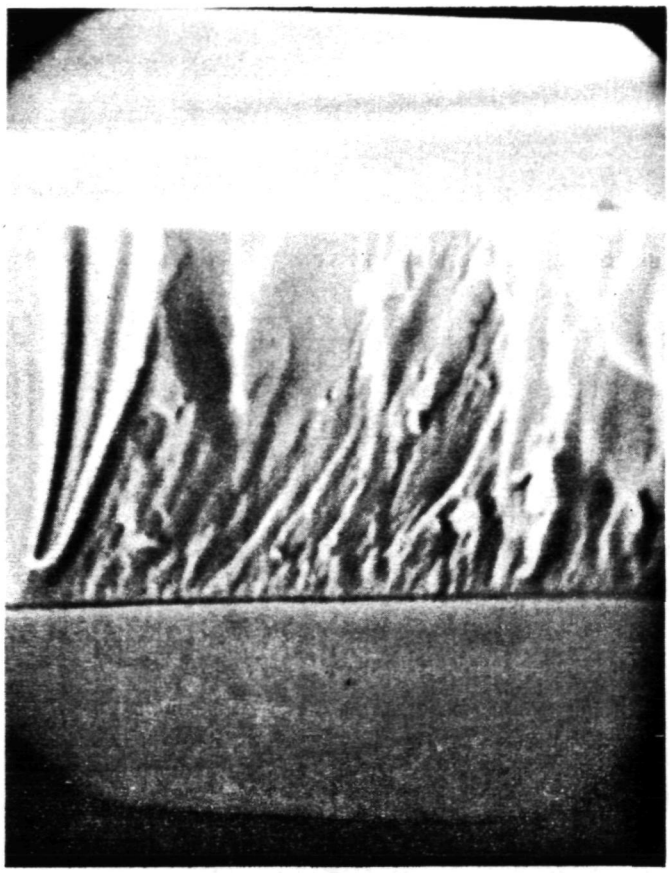

Figure 1: Magnified cross section of a film of poly(p-aminophenylacetylene) on a glass substrate. Magnification 13 500x. Film thickness 3.6 microns.

the solution. Re-stirring the solution and filtering was found to greatly reduce this problem.

4.2 Sandwich devices

Work on thin-film sandwich devices was initiated for two reasons. Sandwich devices with a solid upper electrode (see Figure 2) were used for measurements of basic electrical characteristics (contact behavior, capacitance, conductance). Sandwich devices with a semi-open upper electrode (see Figure 3) were intended to be used for gas detection. Extremely poor yield of these latter devices led to abandonment of this particular device configuration in favor of work with lock-and-key devices.

Thin-film sandwich devices were fabricated by evaporating an aluminum electrode onto a glass substrate, coating the electrode with polymer, and evaporating an aluminum electrode over the polymer. The active device area was on the order of 1 cm^2. For sandwich devices with an open upper electrode, the device was then spin coated with photoresist and baked at 50°C. The resist was then exposed through a mask. The resist was developed, exposing regions of aluminum, which were then etched away, yielding the semi-open upper electrode pictured schematically in Figure 3. A new mask (Figure 4) was made specifically for these devices, but was not used because of yield problems discussed below.

Even without the processing required to obtain an open upper electrode, the yield of good (non-shorted) devices was very poor, on the order of 25% for PPA, PNPA, and PAPA and much less than 25% for other polymers. The

TOP VIEW

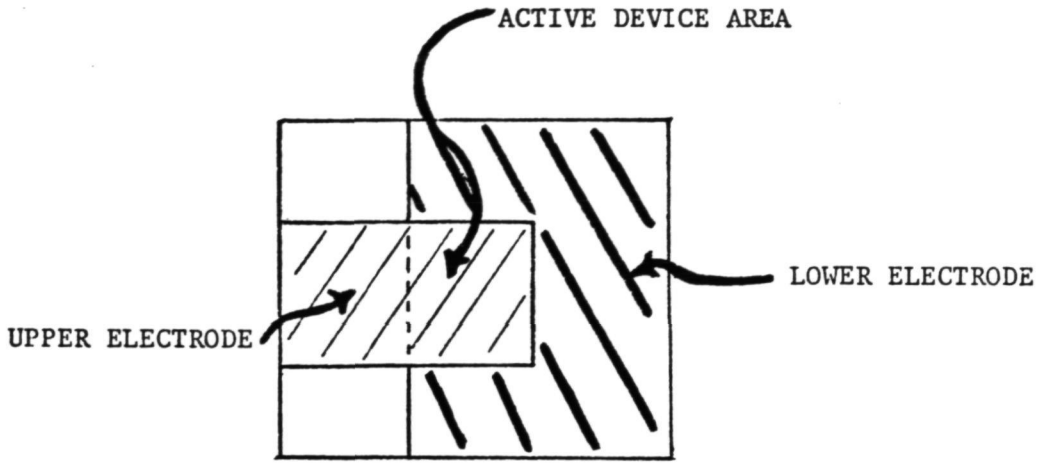

SIDE VIEW (EXPANDED)

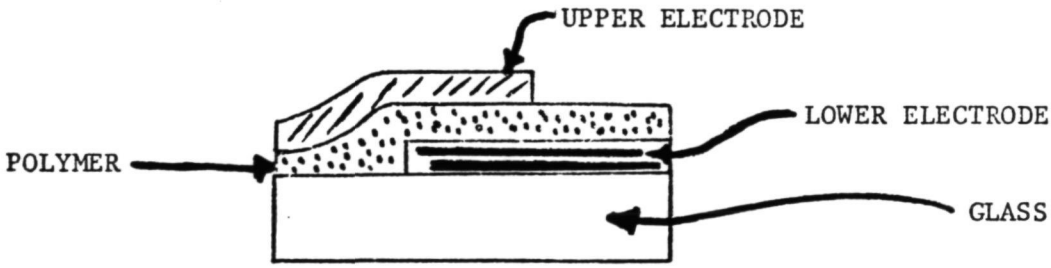

Figure 2: The metal-polymer-metal thin-film sandwich.

TOP VIEW

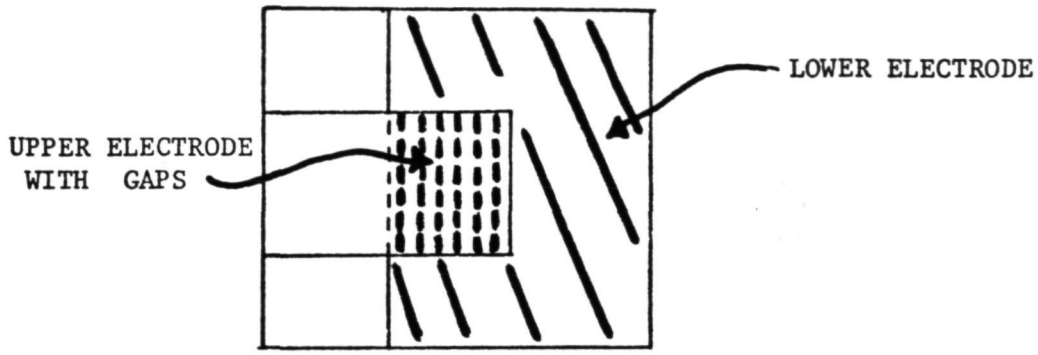

SECTION

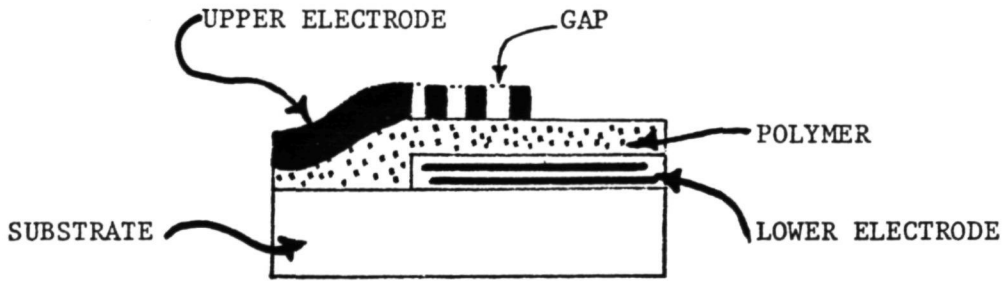

Figure 3: Open-metal-polymer-metal device.

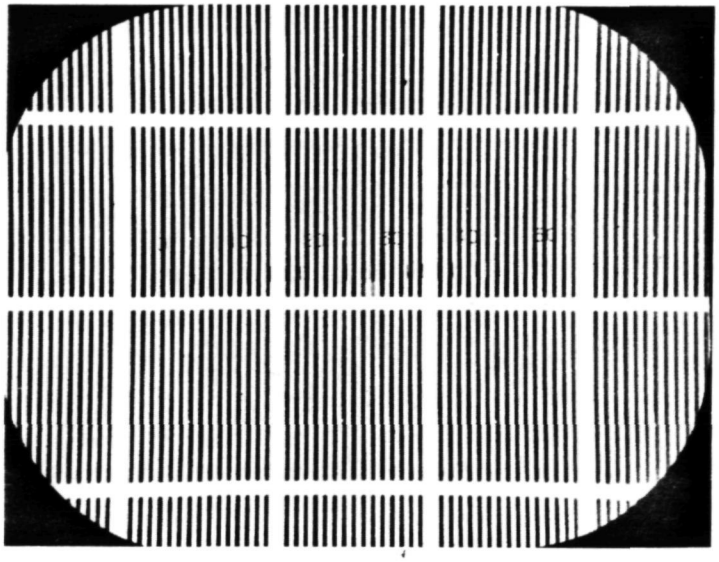

FIGURE 4: A magnified (50 x) section of the mask to be used for the open upper electrode of a metal-polymer-metal sandwich. The dark spaces will be etched out to expose the polymer beneath the upper electrode. The width of each space is approximately 1/2 mil.

reasons for the poor yield are not entirely clear. Certainly, any regions of polymer film that have crystallized might be expected to have short circuits, because when such crystallization occurs, there are cracks and gaps between crystallites, visible under a microscope, into which the aluminum can go during evaporation of the upper electrode. In addition, however, we have observed that some devices which are not shorted immediately after fabrication nevertheless develop short circuits while on the shelf. This phenomenon has been observed with PPA, PAPA, and PEF. An obvious possibility is that the films contain "thin spots", and that either aluminum diffuses through the thin spots producing shorted regions, or the thin spots undergo electrical breakdown so easily that even a delicate probing for a short destroys the device. For example, the typical probe voltage was less than 100 mV (a voltage that does not destroy good sandwich devices). If a thin spot were on the order of 0.1 microns thick, a 100 mV potential would correspond to a field strength of 10^4 volts/cm, which might be capable of producing breakdown. The breakdown hypothesis does not, however, explain <u>why</u> breakdown might become easier as the devices age.

The poor yield of good sandwich devices had two important effects on the program. First, the electrical measurements program was restricted to a total of forty devices and to four polymers: PPA, PNPA, PAPA, and PFPA. (A fifth polymer (PEF) was used for sandwich devices that tested as "good" immediately after fabrication, but which were always shorted by the time electrical measurements were attempted, usually within a day.) Second, the

low yield made work on open-upper-electrode devices totally impractical, and no useful open-upper-electrode devices were obtained. (A lone non-shorted open-upper-electrode device did survive. It, however, was coated with PPA, a polymer that was later found to form blocking contacts with aluminum. It could not, therefore, be used for gas tests.)

One important problem in device fabrication concerns whether the polymer films can survive the processing steps that are needed to define a patterned upper electrode. The capability to survive these processing steps is essential for any device configuration, including field-effect devices, that requires patterned metallization over the polymer. Five of the polymers (PPA, PNPA, PAPA, PFPA, and PEF) were subjected to the following patterning test: A glass slide was coated with polymer, and an aluminum coating was evaporated over the polymer. This aluminum layer was then coated with photoresist, and a semi-open electrode pattern was then defined in the resist and the aluminum in the inter-electrode gaps was etched away. The test was simply whether the polymer film remained intact through the processing steps. Of the five polymers tested, only the formamido polymer (PFPA) failed to survive. The other four polymers were still present on the substrate after etching, although the amino and nitro polymers showed a tendency to separate from the substrate, this separation being produced in the final water rinse following etching. A final processing step, the removal of the photoresist from those areas of aluminum not etched away, was found to destroy all the polymers. This means that before these polymers could be used in production devices that required

patterning over the polymer, resist removal methods would have to be carefully examined.

The combination of the difficulty of producing non-shorted sandwich devices, coupled with the apparent need for careful study of resist removal, led to the conclusion that it is far preferable to work with device configurations in which polymer application is done as a final step, after all other device processing is complete.

4.3 Lock-and-key devices

The lock-and-key device consists of two interdigitated aluminum finger electrodes coated with polymer (see Figure 5). Each finger is 4 mils wide, and the gap between alternate fingers is 6 mils. One electrode has 43 fingers, the other 42, yielding a total of 84 inter-finger gaps 6 mils wide and 0.76 inches long.

The devices are prepared by evaporating aluminum ($\sim$0.4 microns thick) onto a cleaned and degreased microscope slide, coating the aluminum with photoresist, defining the pattern for the electrodes in the photoresist, and then etching away the aluminum to form the gap between electrodes. Care must be taken to etch all of the aluminum out of the gap. The devices are then spin-coated with polymer from solution.

The fabrication steps are routine, and a high yield of good devices is obtained. In vacuum, the lock-and-key devices have conductances on the order of 5×10^{-14} mhos prior to coating with polymer. A total of 70 lock-and-key devices have been used for various gas and fire tests, including at least three devices for each NASA supplied polymer.

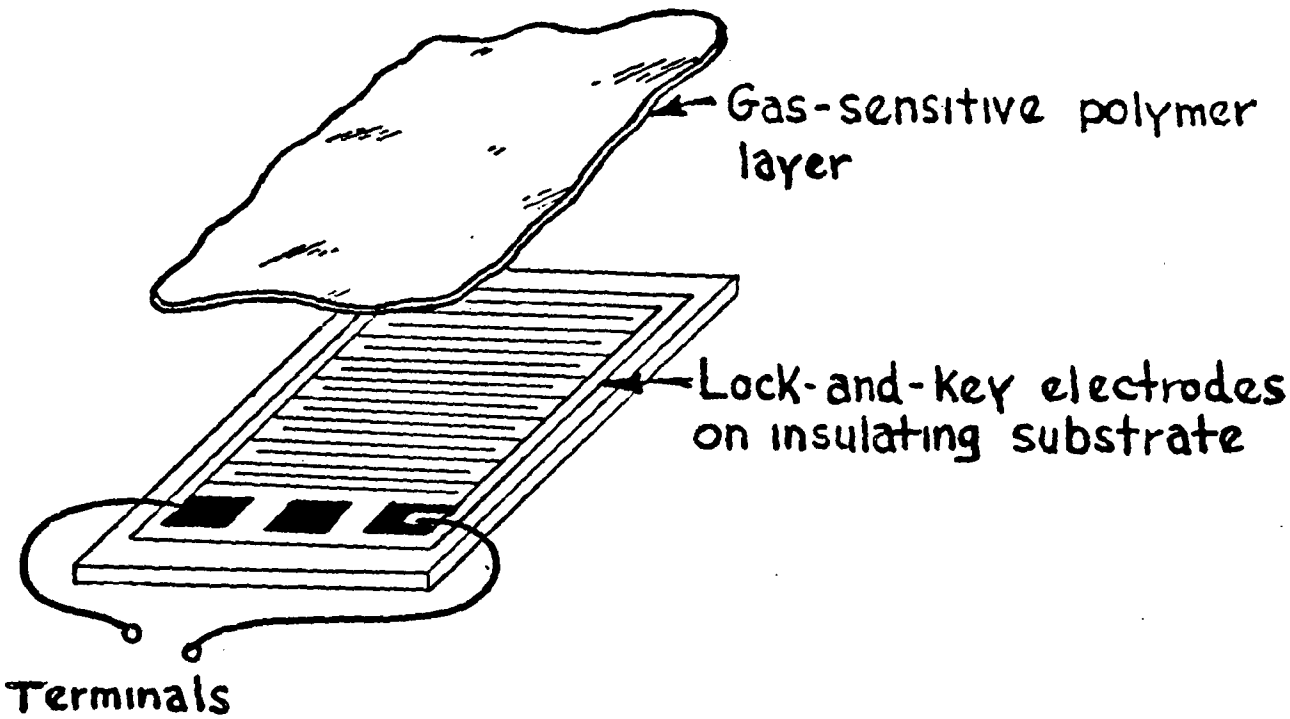

Figure 5: Lock-and-key Device.

CHAPTER 5 THEORETICAL MODELS OF DEVICE OPERATION

This chapter presents a theoretical model of device operation in terms of phenomenological properties of the polymer: conductance and dielectric permittivity. It is assumed that all contacts to the polymer are ohmic, and that the polymer is linear and isotropic.

5.1 Sandwich devices

If a polymer film of thickness T is placed between two metal electrodes of area A (see Figure 2), an equivalent circuit for such a device (neglecting edge effects) is a conductance G in parallel with a capacitance C, where

$$G = \frac{A}{T} \sigma_p \qquad 5.1$$

and

$$C = \frac{A}{T} \varepsilon_p \qquad 5.2$$

In these expressions, the conductivity of the polymer σ_p is expressed in $(\text{ohm cm})^{-1}$ and the dielectric permittivity ε_p in farads/cm.

In the devices used in this study, T is on the order of one micron (10^{-4}cm), while A is on the order of 1 cm^2. From geometry alone, therefore, one would not expect edge effects to be significant in these devices unless there happened to be a large leakage current around the polymer film. The fact that large conductances are observed for some polymers and small conductances for others suggests that leakage paths are not dominant. In addition, experience with lock-and-key devices, where leakage paths are

important, indicates that in sandwich devices the maximum contribution of leakage paths to the total device current must be small compared to the current through the polymer film.

If the contacts are ohmic (as indicated by a linear current-voltage characteristic for the sandwich device), then the ratio of C to G is the dielectric relaxation time of the polymer:

$$\frac{C}{G} = \frac{\varepsilon_p}{\sigma_p} = \tau_p \qquad 5.3$$

One useful test of device-to-device consistency is the reproducibility of this ratio for nominally identical devices.

5.2 Lock-and-key devices

A quantitative model of the lock-and-key device is developed in Appendix A. That model includes a simplifying geometrical assumption, that the width of the fingers and the width of the gaps between fingers are identical. In practice, the fingers are 4 mils wide and the gaps are 6 mils. In the model both are assumed to be 5 mils, an approximation that is sufficiently accurate for the present purposes.

The results of Appendix A state that the equivalent circuit for the lock-and-key device of area NLW, where N is the number of gaps, L is the center-to-center distance for adjacent fingers (10 mils) and W is the length of the fingers (0.76 cm), coated with a polymer of thickness T, is a conductance G in parallel with a capacitance C where

$$G = 0.8 \frac{NW\ 4\ \sqrt{2}}{\pi^2} \{ \frac{\pi}{L} (\kappa_p + \kappa_g) + \sigma_g + \frac{\pi T}{L} \sigma_p \} \quad 5.4$$

and

$$C = 0.8 \frac{NW\ 4\sqrt{2}}{\pi^2} \{ \varepsilon_0 + \varepsilon_g + \frac{\pi T}{L} \varepsilon_p \} \quad 5.5$$

In the above expressions, σ_p and ε_p are the conductivity and permittivity of the polymer, σ_g and ε_g are the conductivity and permittivity of the glass substrate, ε_0 is the permittivity of free space, and κ_p and κ_g are the surface conductivities of the glass-polymer and polymer-air interfaces, respectively, (see Figure 6). Two features of these equations are important. First, because $T/L << 1$, the conductance could easily be dominated by the surface conductivities of the glass or of the polymer. The conduction paths, and an equivalent formula for the conductance are illustrated in Figure 7. Second, the dielectric permittivity of the polymer would have to be enormous in order for the presence of the thin polymer coating to modify the measured capacitance.

The expressions for conductance and capacitance are used in the interpretation of electrical measurements, gas-test data, and fire-tests data. In the chapters that follow, it is useful to recognize that conductance effects which increase with increasing polymer thickness (hence with increasing solution concentration) are likely to be associated with the bulk conductivity of the polymer, while effects that are unaffected by the polymer thickness are likely to be associated with other terms in the conductance expression.

LOCK-AND-KEY : ELECTRICAL PARAMETERS

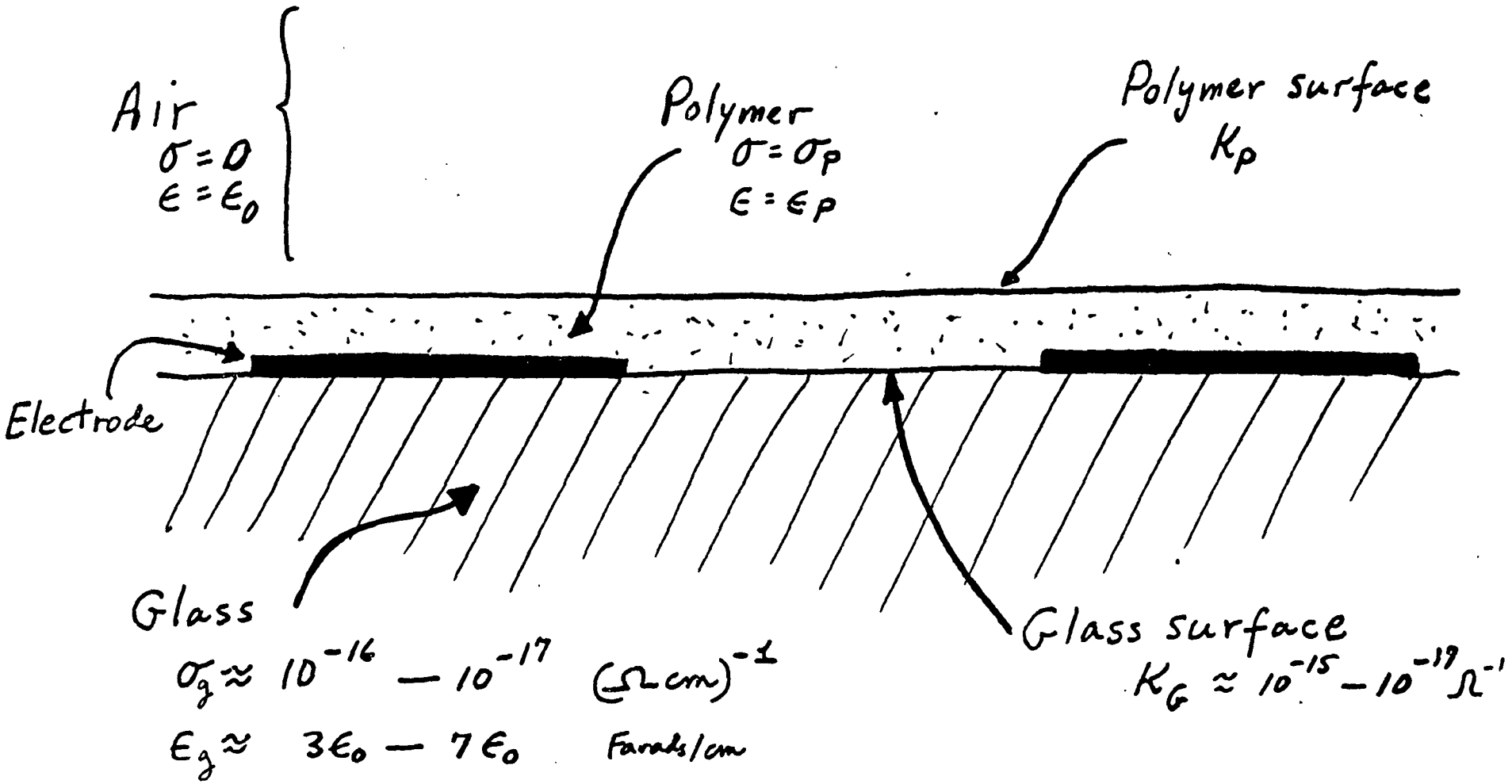

Figure 6

LOCK-AND-KEY : CONDUCTION PATHS

$$G \approx 1.5\left(\frac{NW}{L}\right)\left\{K_G + K_P + \sigma_G \frac{L}{\pi} + \sigma_P T\right\}$$

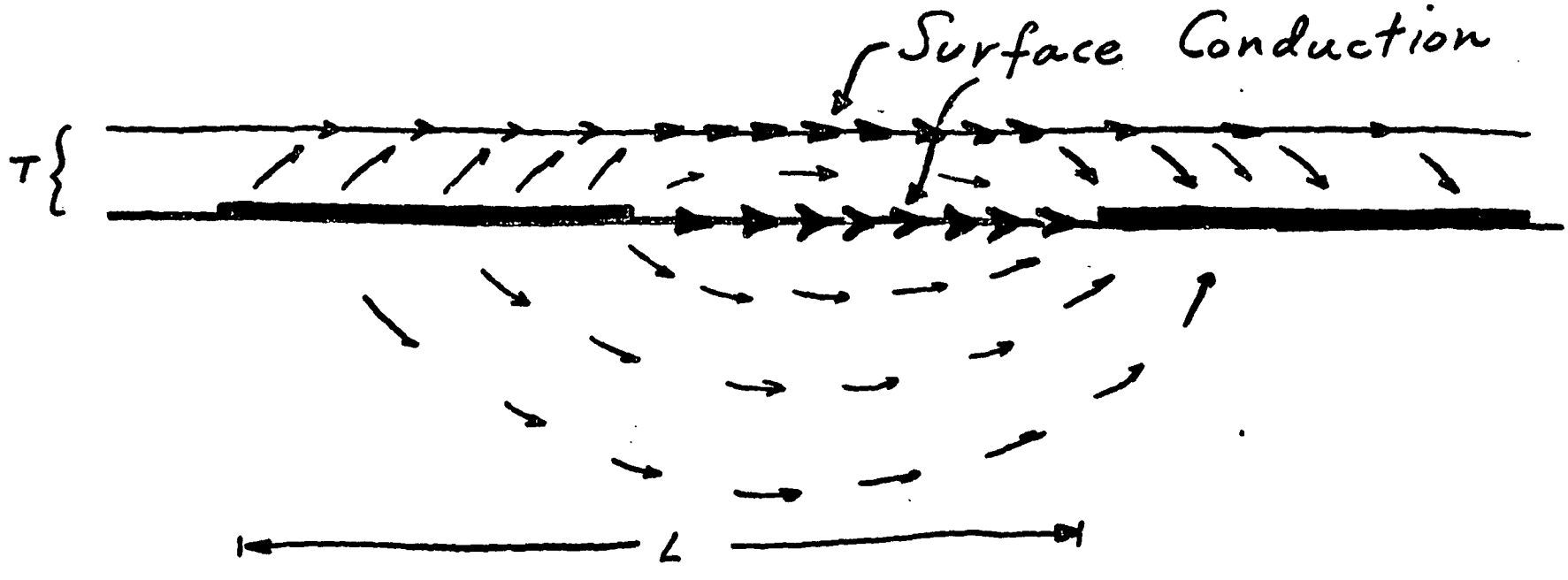

Figure 7

CHAPTER 6 ELECTRICAL MEASUREMENTS

6.1 Methods

Figure 8 shows the circuit configuration used for measuring dc current-voltage characteristics of both thin-film-sandwich and lock-and-key devices. A variable source voltage (0-5 volts for sandwich devices, 0-50 volts for lock-and-key devices) is connected in series with a Keithley model 610 C electrometer (used as a picoammeter) and the device under test. The source voltage is measured with a Hewlett-Packard model 3440 A digital voltmeter. When needed, a correction to this measured voltage to account for the non-zero voltage drop across the electrometer was used. This correction was particularly important when measuring sandwich devices in voltage ranges below 1 volt. Both the device under test and the voltage source were fully shielded from outside electrical interference.

Capacitance measurements were made with a General Radio model 1620-AP capacitance bridge assembly, operating in the range 50 Hz - 10 kHz. Most measurements were made at 1 kHz. Of the polymers tested, only the amino polymer (PAPA) showed a frequency-dependent capacitance. For this polymer, measurements were made as a function of frequency.

The effect of temperature was studied in a few cases. This was done by placing the sample holder in a lab oven. Oven temperature was monitored with a thermocouple. All measurements of temperature dependence were at temperatures above room temperature, and were carried out in ambient laboratory air to a maximum temperature of about 100°C.

For one of the polymers, PNPA, it was possible to measure the

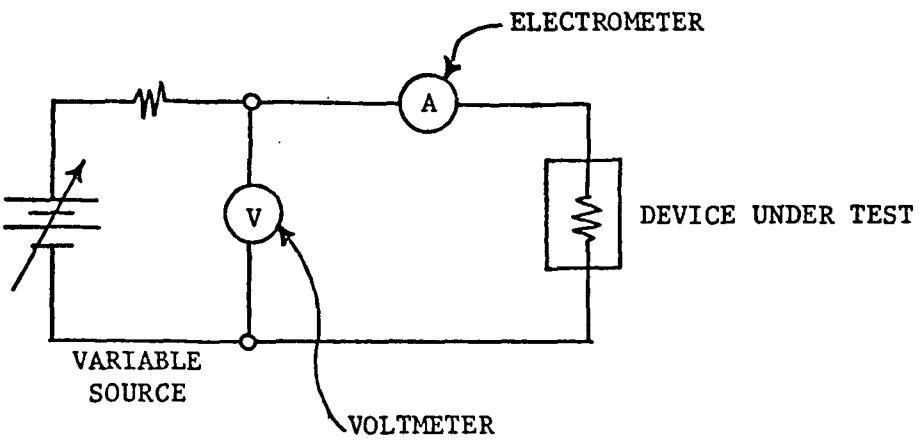

Figure 8: Circuit for measuring current-voltage characteristics

frequency dependence of the conductance of a thin-film sandwich device directly from the capacitance bridge. In most cases, however,the dielectric loss at audio frequencies was so small that no useful ac measurements of shunt conductance could be made.

6.2 Contact linearity

Aluminum forms blocking contacts with PPA (see Figures 9 and 10) and linear contacts with PNPA and PAPA (see Figures 11 and 12). In the case of PPA, the non-linearity is exponential, a characteristic typical of Schottky barriers. In the case of PAPA and PNPA, the current-voltage characteristic is linear right down to the origin (the lower limit on measurements actually made on a PAPA device is 5 millivolts). Departures from linearity at higher currents for PNPA and PAPA are typical of space-charge-limited currents in weak conductors. No current-voltage measurements could be made on thin-film sandwiches for the remaining five polymers; the one non-shorted PFPA device failed after capacitance measurements were completed.

6.3 Capacitance measurements

As stated in Chapter 5, the capacitance of lock-and-key devices is virtually insensitive to the dielectric constant of the polymer. Equation 5.5, when evaluated for our device geometry and for a dielectric constant of 5 for glass, yields a lock-and-key capacitance of about 40 pF, a number that is in good agreement with our experimental results, which were

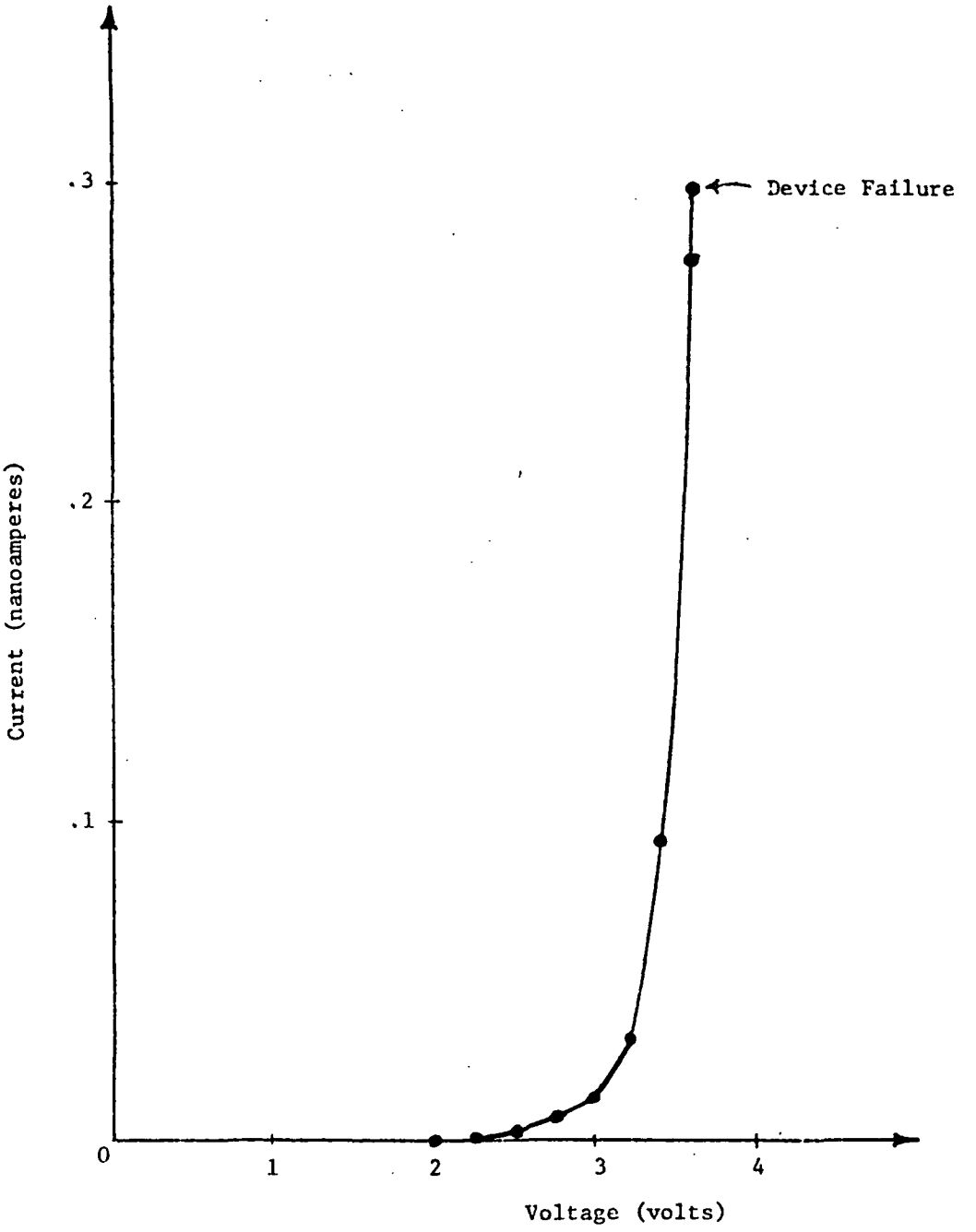

Figure 9: Current-voltage characteristic of a sandwich device (3-1-2) with poly(phenylacetylene) between aluminum electrodes.
The nonlinearity is similar to that of a Schottky-barrier diode.

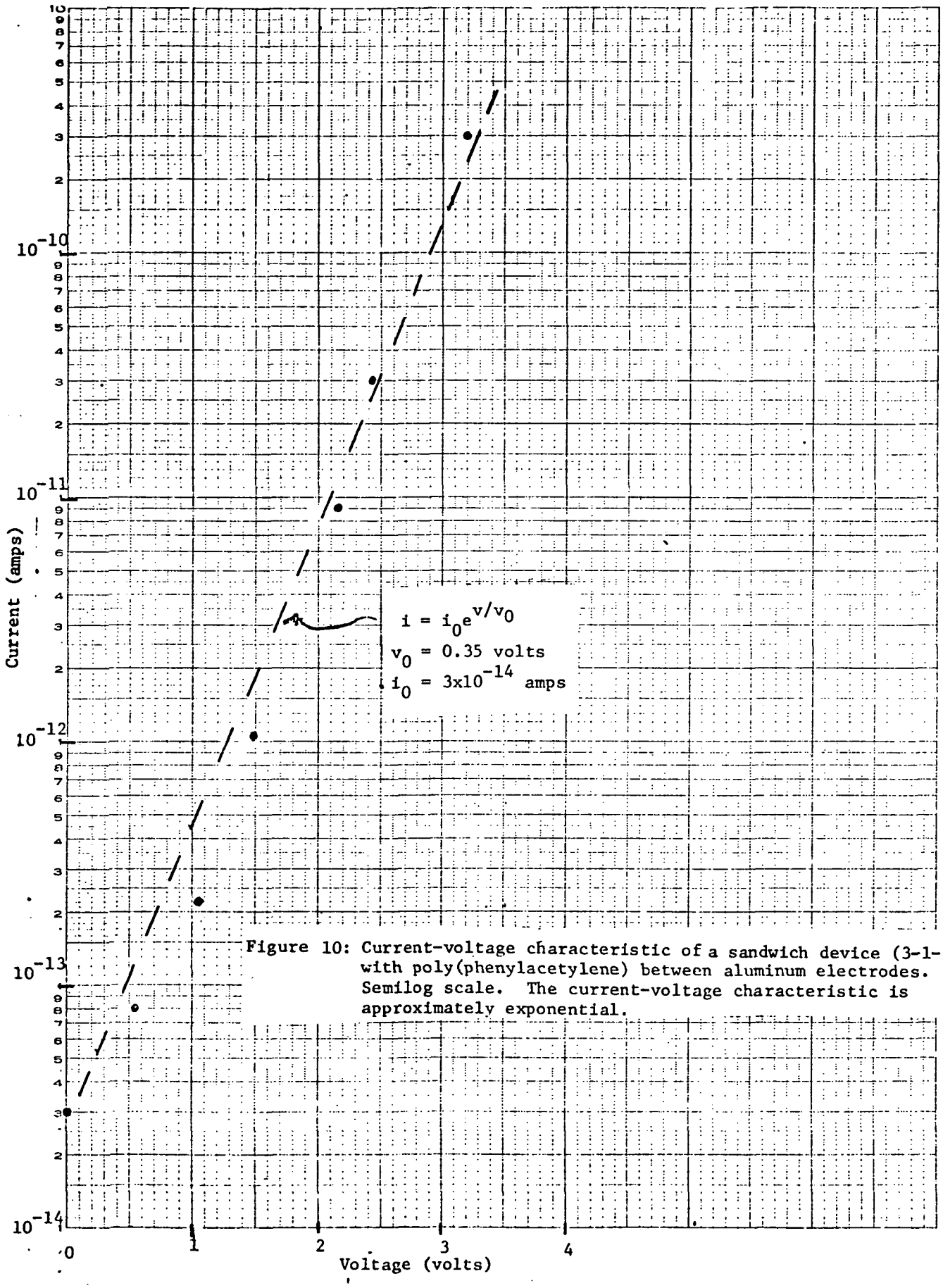

Figure 10: Current-voltage characteristic of a sandwich device (3-1-1) with poly(phenylacetylene) between aluminum electrodes. Semilog scale. The current-voltage characteristic is approximately exponential.

Figure 11: Current-voltage characteristic of a sandwich device (3-16-2) with poly(p-nitrophenylacetylene) between aluminum contacts.

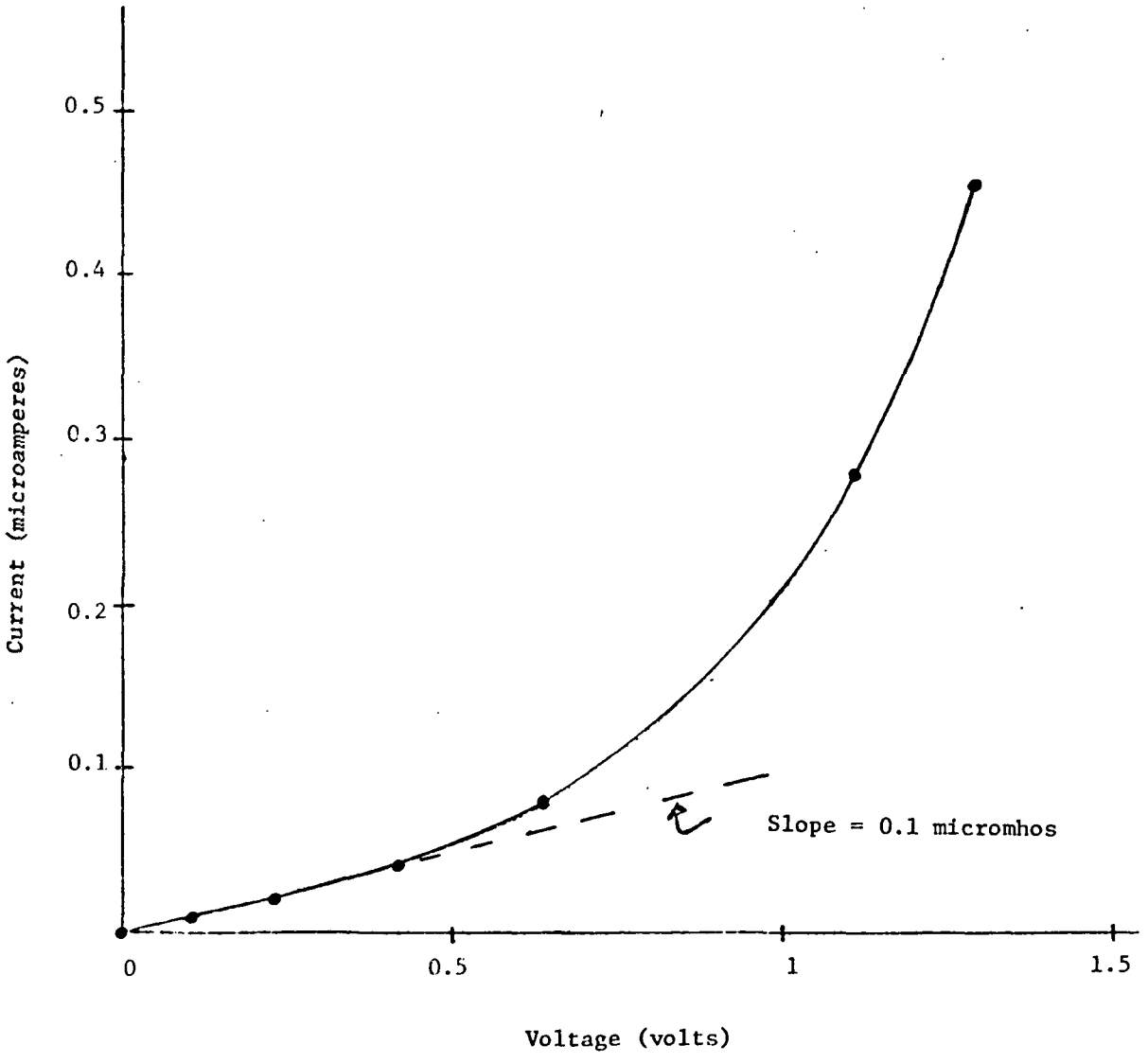

Figure 12: Current-voltage characteristic of a sandwich device (3-6-2) with poly(p-aminophenylacetylene) between aluminum contacts. The Ohmic (linear) behavior at low voltages shows the absence of a Schottky barrier.

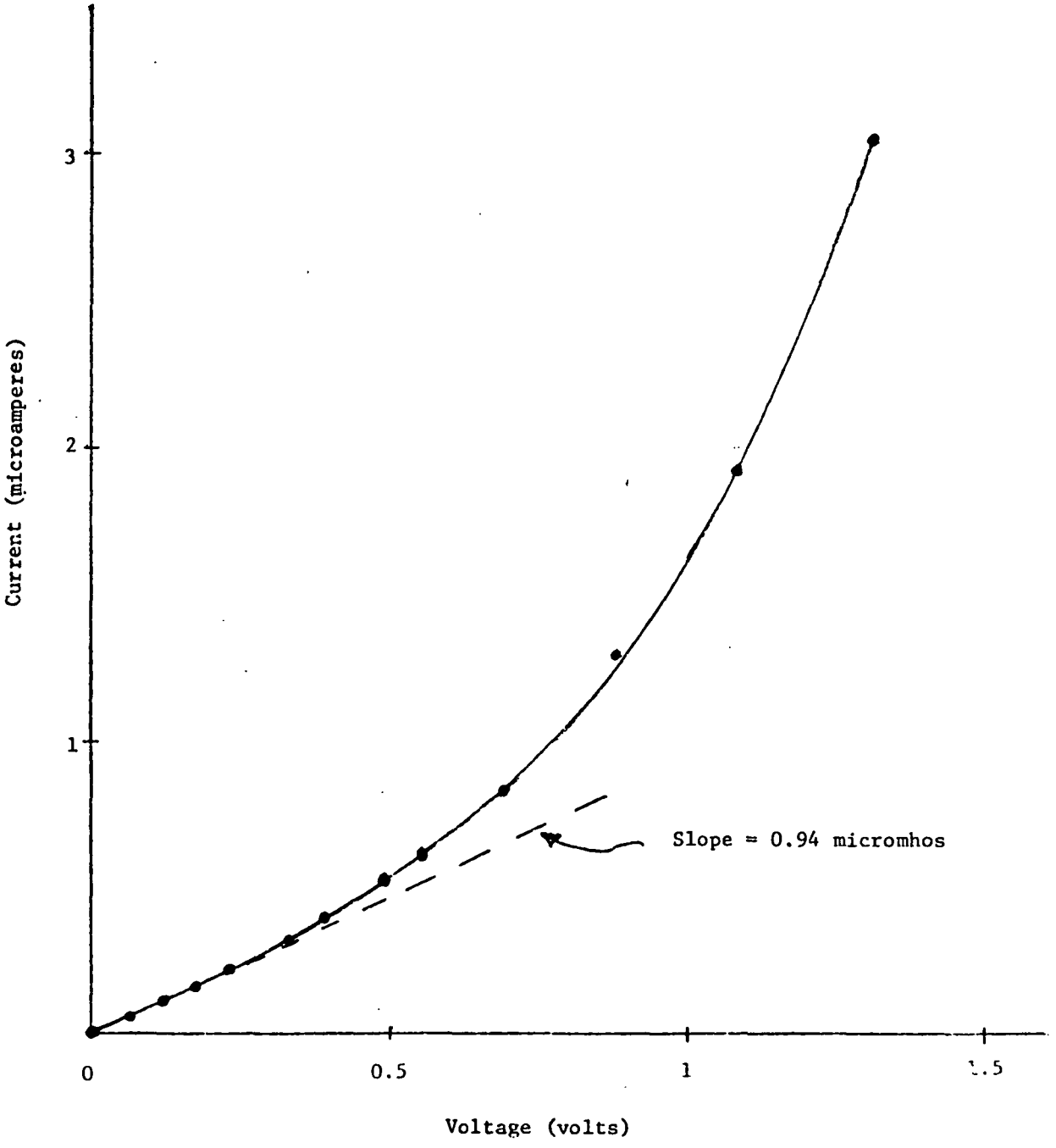

in the range 35-60 pF. Because of the relative insensitivity of the capacitance to variations in polymer film, most capacitance measurements were made on the thin-film sandwich devices.

The capacitance data for thin-film sandwich devices are summarized in Table II. Within a given batch of devices (the second number of the three-number device code represents the batch), the capacitance per unit area is quite reproducible for all but the amino polymer. This suggests that similar processing will indeed yield reproducible device characteristics.

It is interesting that there are almost two orders of magnitude of variation between PPA and PAPA, suggesting strong variations of dielectric constant from polymer to polymer. Because precise thickness data were not obtained for all polymers, it was only possible to estimate a dielectric constant using film thickness data appropriate to PAPA. For those film-thickness values, and relying on the 20% solutions where possible (because of the thicker films, hence possibly more reliable data), estimated dielectric constants of about 12, 19, and 300 are obtained from PPA, PNPA, and PAPA respectively. The single estimate for PFPA is 182. While it must be emphasized that these are only estimates, the relative dielectric constants obtained here correlate very closely with the observed sensitivity of these various polymers to the fire test. As discussed in Chapter 8 to follow, Both PAPA and PFPA respond well to the fires, PNPA responds much less well, and PPA hardly responds at all.

One additional interesting result can be obtained from a comparison of the capacitances of devices 3-4-3 and 3-4-5, and also of devices 3-13-1 and 3-13-2. These pairs of devices differ only in the spinning

TABLE II

ELECTRICAL MEASUREMENTS ON THIN FILM SANDWICH DEVICES

POLYMER		DEVICE NUMBER	AREA $(cm)^2$	CAPACITANCE/AREA ($\mu F/cm^2$)	FREQUENCY (kHz)	ESTIMATED DIELECTRIC CONSTANT* ($\varepsilon_p/\varepsilon_0$)	CONDUCTANCE/AREA ($\mu S/cm^2$)	ESTIMATED RESISTIVITIES* (Ω -cm)	TIME CONSTANT (seconds)
PPA	20% solution 6000 rpm	3-0-3	2.26	.0022	1	9	–	–	–
	" "	3-0-4	2.10	.0023	1	9	–	–	–
	" "	3-0-5	1.92	.0041	1	17	–	–	–
	" "	3-0-6	1.78	.0036	1	15	–	–	–
	" "	3-1-1	1.59	.0031	1	13	–	–	–
	" "	3-1-2	1.44	.0031	1	13	–	–	–
	" "	3-1-3	1.58	.0031	1	13	–	–	–
	" 4000 rpm	3-4-3	1.88	.0022	1	9	–	–	–
	" 9000 rpm	3-4-5	1.64	.0033	1	13	–	–	–
	4% solution 6000 rpm	3-2-1	1.87	.022	1	22	–	–	–
	" "	3-2-2	1.73	.021	1	21	–	–	–
	" "	3-2-4	1.57	.021	1	21	–	–	–
	" 2000 rpm	3-13-1	2.43	.013	1	13	–	–	–
	" 3000 rpm	3-13-2	2.60	.018	1	18	–	–	–
	" 2 coats	3-14-1	2.67	.018	1	18	–	–	–
	" 3 coats	3-14-3	2.37	.018	1	18	–	–	–
PAPA	5% solution 6000 rpm	3-6-2	2.13	.310	0.1**	350	.44	2.4×10^{10}	.70
	" "	3-6-5	2.01	.240	0.1	280	6.0	1.6×10^{9}	.04
	4% solution 6000 rpm	3-8-2	1.77	.270	0.1	310	.20	5.4×10^{10}	1.35
PNPA	20% solution "	3-16-1	2.43	.0046	1	19	–	–	–
	" "	3-16-2	2.54	.0045	1	19	.029	9.5×10^{10}	.16
	" "	3-16-3	2.89	.0046	1	19	.032	8.6×10^{10}	.14
	" "	3-16-4	2.88	.0048	1	19	–	–	–
	4% solution "	3-3-1	1.81	.032	1	32	.055	2.0×10^{11}	.58
	" "	3-3-2	2.03	.027	1	27	–	–	–
	" "	3-3-3	2.15	.031	1	31	.054	2×10^{11}	.57
	" "	3-3-4	2.69	.023	1	23	.46	2.4×10^{10}	.05
	" "	3-3-5	2.08	.032	1	32	.010	1.1×10^{12}	3.1
PFPA	4% solution "	3-10-2	1.63	.178	1	182	–	–	–

*Estimated dielectric constants and resistivities assume uniform film thickness of 3.63 μ (20%), 0.96 μ (5%), and 0.91 μ (4%) for all polymers

**The capacitance of PAPA devices was frequency dependent. For these devices C(1 kHz)/C(0.1 kHz) $\approx$ 2/3

speed used to apply the polymer. In each case, the device with the higher spinning speed has the higher capacitance. Since higher speed might be expected to yield thinner films, this variation with spinning speed is not unreasonable.

As a final comment on the capacitance data of Table II, attempts at multiple coatings (devices 3-14-1 and 3-14-3) did not yield any change in capacitance.

Only the amino polymer exhibited a frequency-dependent capacitance. The frequency dependence of the PAPA capacitance is shown in Figure 13. The figure shows total capacitance rather than capacitance-per-unit-area. The dependence on frequency of all four curves is similar,with the dielectric constant decreasing by a factor of two between 50 Hz and 10 kHz. It is evident from the data that there is a dielectric relaxation at frequencies somewhat below 50 Hz, of which the data in Figure 13 represent the high-frequency dispersive tail. Normally, one would expect some associated peaking in the conductance at frequencies corresponding to the relaxation time. The absence of capacitance and conductance data in the sub-audio range prevents our being able to do further investigation of this phenomenon.

The capacitance measurements did yield frequency-dependent conductance data for PNPA, as shown in Figure 14. The linear increase of conductance with frequency above 50 Hz suggests hopping conduction as a mechanism. For reference, the dc conductance value for this device is indicated in the figure.

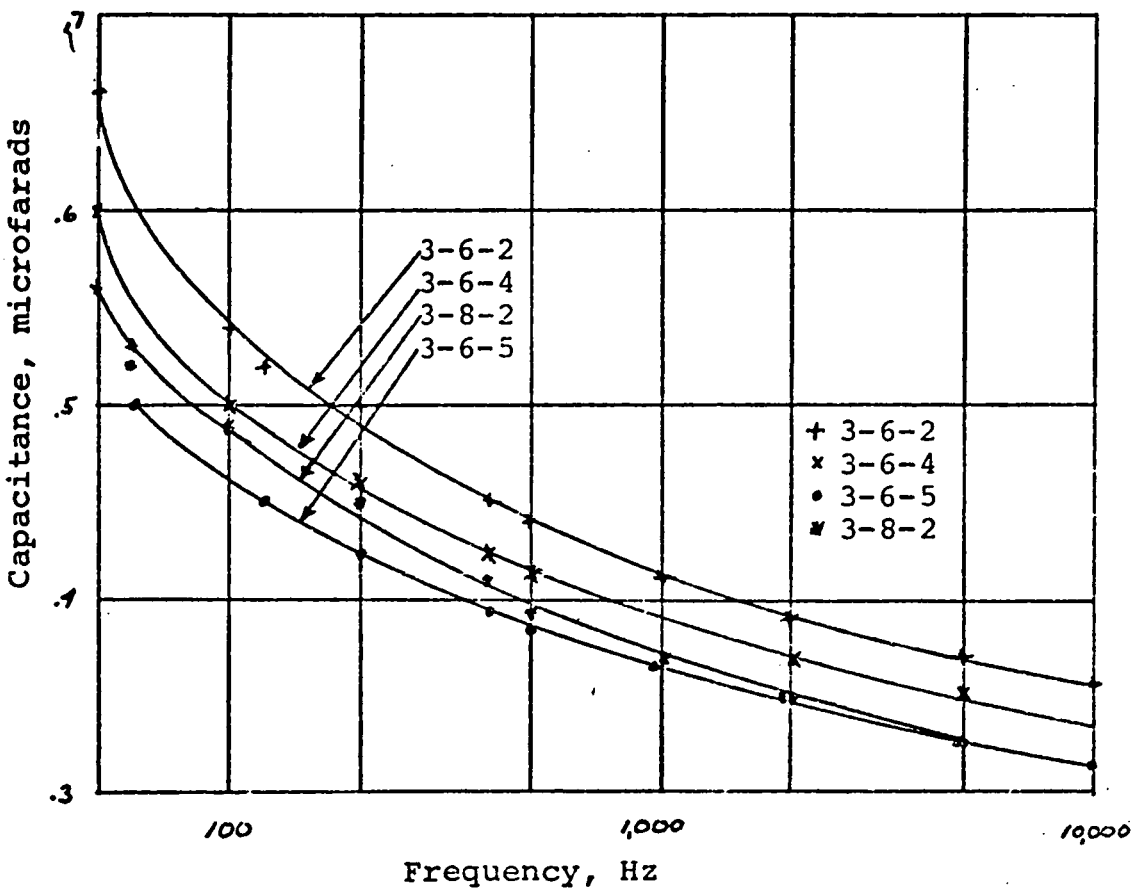

Figure 13: Capacitance vs. frequency for sandwich devices made with PAPA

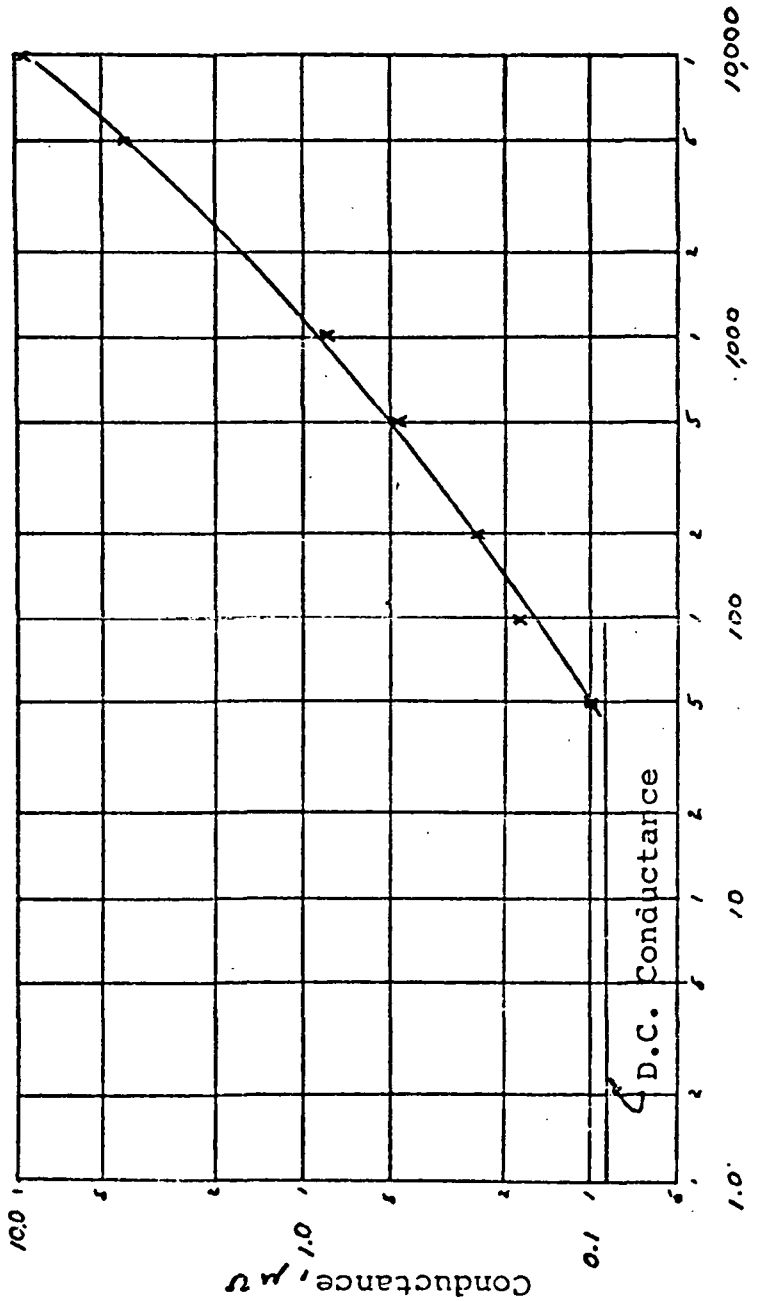

Figure 14: Conductance vs. frequency for device 3-16-4, 20% PNPA

6.4 Conductance measurements

The dc conductance measurements for thin-film sandwich devices and for lock-and-key devices in vacuum were hampered by two problems. First, the data for the thin-film sandwich devices were highly non-reproducible, as evidenced in Table II.* In contrast with the capacitance data, devices within a single batch do not have equivalent conductances (the conductance data in Table II are taken from the linear portion of the current-voltage characteristic, and not from the space-charge-limited region).

It is believed that this lack of reproducibility may be due to thin spots in the polymer films. Under dc conditions, the thin spots will carry most of the current, and will therefore heat slightly, which will, in turn, tend to increase either the conductance of the thin spots or the efficiency of carrier injection into the thin spot regions. Indeed, even films that show stable current-voltage behavior at low currents develop instabilities at higher currents that resemble the onset of thermal runaway.[7] If the dc conductance were dominated by thin spots or by the enhancement of thin spot conductance due to local heating, then one might expect that the average resistivity calculated assuming no thin spots would be very much too small. As Table II shows resistivities estimated from assumed ideal device geometry fall in the range of 10^9 to 10^{12} Ohm-cm. These are much smaller than expected on the basis of other data, as discussed below.

---

*The PPA devices have blocking contacts, so no meaningful conductance data are obtained.

The time constants for the devices that have conductance data also show a lack of reproducibility, and since the device geometry should cancel out for the time constant, this lack of reproducibility suggests even more strongly that under dc conditions, local heating or non-ohmic carrier injection that does not happen under the ac conditions present during a capacitance measurement are responsible for a conductance that is not simply related to the bulk resistivity of the polymer.

One indication that the resistivities estimated in Table II are much too low is obtained from a comparison with the conductance data for lock-and-key devices. From Eq. 5.4, the conductance of a lock-and-key device is given approximately by

$$G = 10^4(\kappa_G + \sigma_{g\pi}\frac{L}{} + \kappa_p + \sigma_p T)$$

In the absence of a polymer coating, the conductance will be determined entirely by κ_g and σ_g. High-resistivity glass has a bulk conductivity on the order of 10^{-17} $(\text{ohm-cm})^{-1}$. Furthermore, a clean glass surface has a surface conductivity of the same order of magnitude[8]; that is

$$\kappa_g \approx 10^{-17}\ \Omega^{-1}.$$

With these estimates, we would expect

$$G \approx 10^{-13}\ \Omega^{-1}$$

for an uncoated electrode <u>in vacuuo</u>, a prediction in excellent agreement with our experimental findings.

When the lock-and-key devices are coated with polymer, we still find

$$G \approx 10^{-13}\ \Omega^{-1}$$

indicating that the contribution of σ_p or of κ_p is small compared to 10^{-17}.

This result in turn suggests that since $T \tilde{\gtrsim} 10^{-4}$ cm, σ_p cannot be as large as $10^{-13}(\Omega\ \text{cm})^{-1}$. Equivalently, the polymer resistivity would have to be greater than $10^{13}\ \Omega$cm, in direct contradiction of the estimates in Table II. These differences in estimates of σ_p cannot be easily reconciled, and it is the conductance data from the thin-film sandwiches in Table II that are suspect.

The temperature dependence of device conductances have been measured for a few thin film sandwich devices and for a few lock-and-key devices. The results are surprising in several ways. Figure 15 shows the effect of heating and cooling a thin-film sandwich device coated with PNPA from room temperature to almost 100°C. As temperature is increased above room temperature, there is initially no variation in device conductance. When the temperature reaches 85°C, the conductance begins to climb. Subsequent cooling yields a conductance lower than the original conductance. These data indicate that before the heating cycle, the PNPA was behaving as a doped semiconductor (in which conductivity is a weak function of temperature), and that after heating above 85°C, the material becomes intrinsic. The cooling cycle suggests that the "dopant" may be a gaseous component that is driven off during heating. This suggests that it may be possible to regenerate devices with a periodic heat cycle.

An equally interesting response was obtained in PEF [poly(ethynyl ferrocene)]. The conductance of a lock-and-key device coated with PEF is shown in Figure 16. The conductance is an exponential function of temperature during heating, but once 85°C is reached, the current-versus

Figure 15: Effects of thermal cycling on the conductance of a thin film PNPA [poly(p-nitrophenylacetylene)] metal-polymer-metal sandwich device (no. 3-3-1).

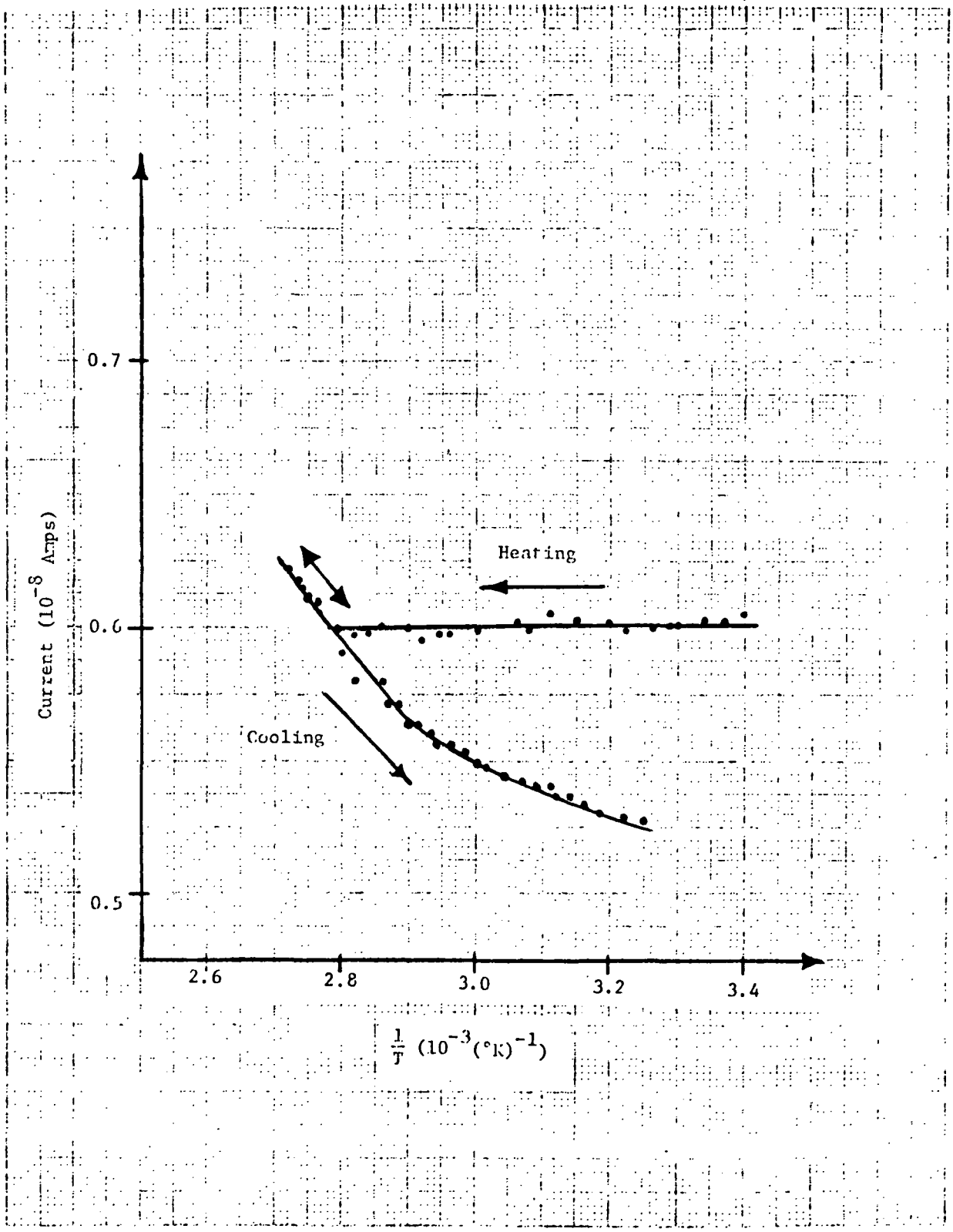

Figure 16: Effects of thermal cycling on the conductance of a lock-and-key device (no. 1-6-1) coated with PEF [poly(ethynyl ferrocene)].

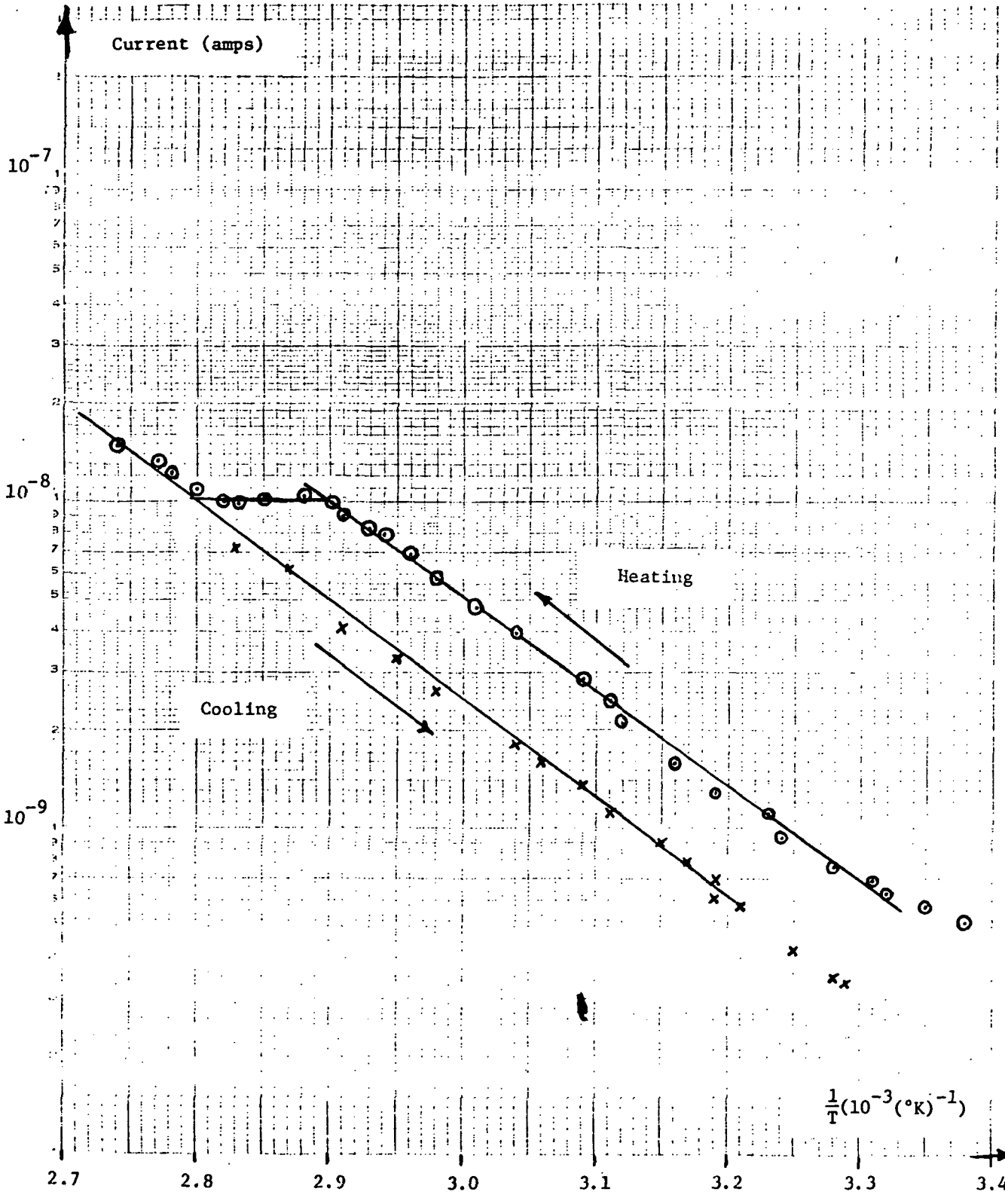

temperature curve shifts to a new exponential with the same activation energy, 0.56 V, but with a pre-exponential factor smaller by a factor of two. After completion of this cycle, the device was left in laboratory ambient overnight. By the following morning, the device had recovered its original conductivity at room temperature.

Both sets of results, and similar results for several other devices, indicate that conductances of these devices do depend on absorbed substances that can be driven off at high temperatures. Water vapor is a prime candidate. A new set of experiments conducted under vacuum are needed in order to ascertain the dynamics of these temperature dependences.

CHAPTER 7 GAS TESTS

7.1 Gas-Test Chamber

A gas-test chamber was designed and assembled for use in this program. Figures 17 and 18 illustrate the design. A bell-jar in which devices can be placed is connected to a mixing manifold and to a port into which as many as three gases can be introduced in a single measurement cycle. In addition, an auxiliary port permits the introduction of dry air, room air, or another gas. The entire chamber was maintained at room temperature. Pressure measurements could be made on any section of the system, using both an MKS Barytron Pressure Transducer, equipped with a 0-100 mm Hg sensing head, and with a Bourdon-tube gage with 0-800 mm Hg range. For most measurements, rough vacuum in combination with repeated flushings with either dry air or dry nitrogen was used to clear the chamber between measurements.

The measurement procedure was as follows: For single gas measurements, the chamber was pumped out and flushed several times with dry air or dry nitrogen. Then measured increments of the appropriate gas were introduced. The current in the lock-and-key device under test, driven with 50 volts dc, was monitored at all times. In cases where the measurements involved a gas in one atmosphere of air, the gas was first introduced its pressure being accurately measured with the MKS gage, then the chamber was filled with air to one atmosphere.

A typical measurement sequence would require a series of measurements at a set of increasing pressures, then the flushing of the chamber to verify

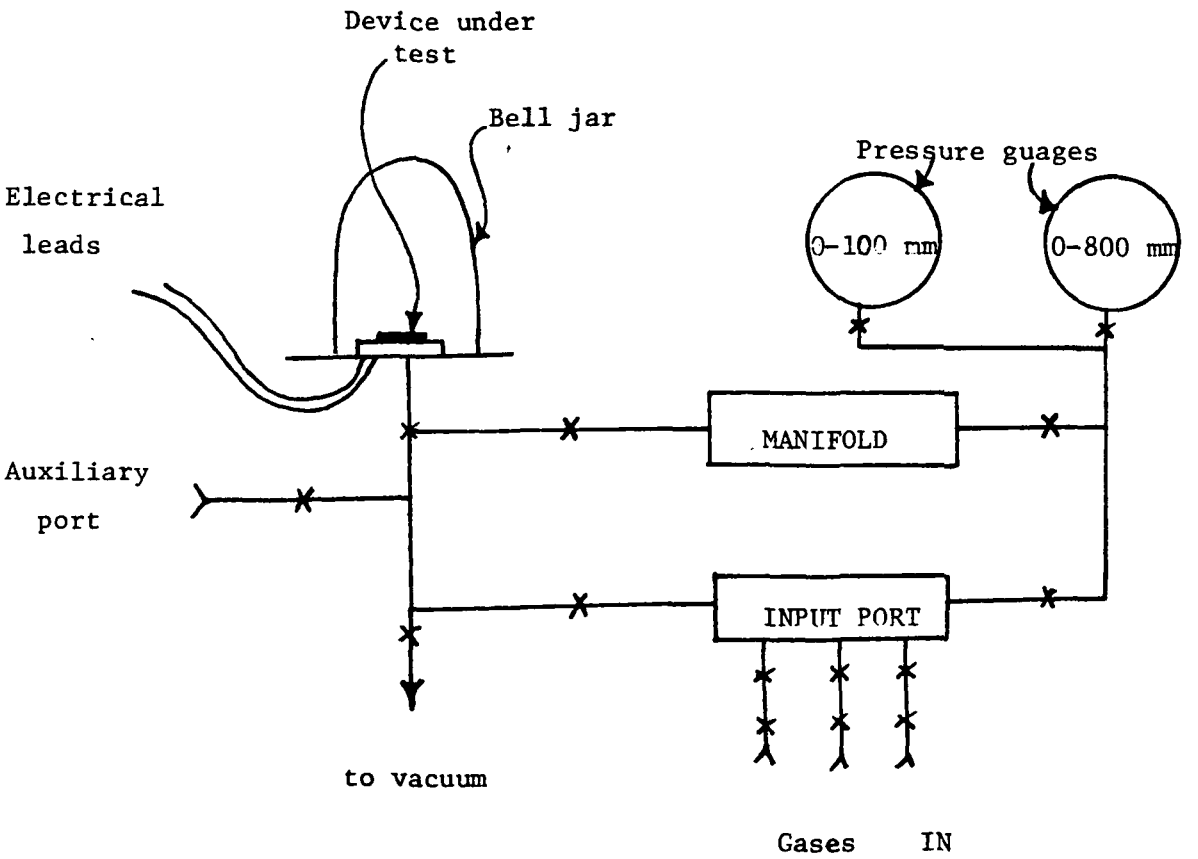

Figure 17: Schematic of gas-test chamber

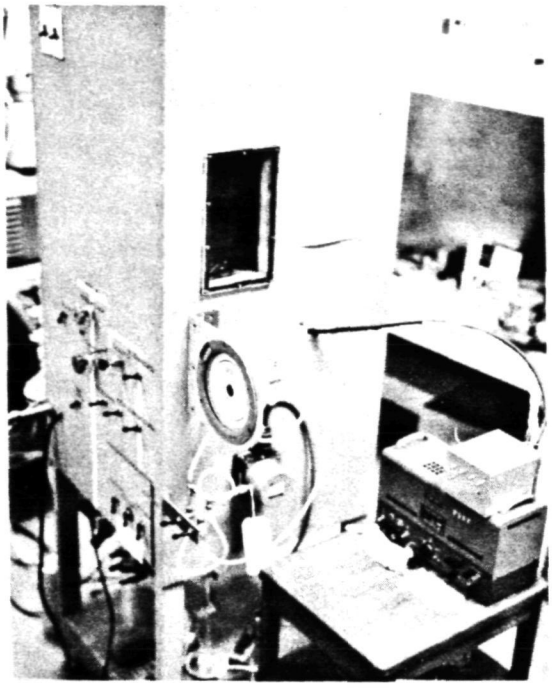

a) Exterior view, showing guages and control panel

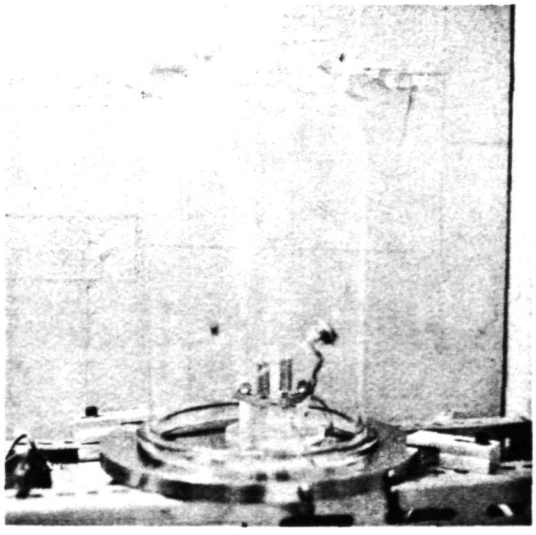

b) Interior view, showing bell jar and probe assembly.

Figure 18: Gas-Test Chamber

that the device conductance returned to its baseline value. Since no devices showed significant responses to dry nitrogen or to dry air, this method was successful in producing a reproducible baseline.

7.2 Tests on Single Gases

The responses of all eight polymers to six different gases were measured, Table III shows the list of gases used and the maximum gas pressures in each case. The acrolein vapor was produced by evaporating liquid into the test chamber through a series of valves to permit controlled amounts to be introduced. All other gases were obtained from commercial research-grade cylinders.

Of the gases tested, only ammonia produced significant responses at low pressures (0-1 mm Hg), and of the remaining gases, only acrolein vapor produced a large response at higher pressures. All other gases showed a roughly linear dependence of device conductance on gas pressure. Table IV tabulates the slopes of these linear dependences, in percent/mm Hg. A hyphen entry represents "no observable response", and means a slope of less than 0.2%/mm Hg. Note that acrolein has a strong response with three polymers, PNPA, PFPA, and PEC. In the case of the nitro and formamido polymers, the response is roughly linear. In the case of PEC, the response is exponential, and is fit by the expression

$$\frac{I}{I_o} = e^{p/p_o} \quad \text{for } p < 20 \text{ mm Hg.}$$

where I_o is the device current in vacuum, and where

$$p_o = 13.8 \text{ mm Hg.}$$

TABLE III

Gases and Maximum Pressures (in mm Hg) used in Single Gas Tests.

Gas	PPA	PNPA	PAPA	PFPA	PEF	PEP	PTMP	PEC
NH_3	50	50	50	56	50	50	50	50
Acrolein	50	50	50	50	50	50	100	50
CO	100	110	50	100	50	50	50	100
SO_2	100	50	50	100	50	50	50	100
CO_2	50	50	50	50	60	50	50	50
C_2H_2	100	50	50	100	50	50	50	50

TABLE IV

Summary of Gas Test Responses in Percent per mm Hg.

GAS	PPA	PNPA	PAPA	PFPA	PEF	PEP	PTMP	PEC
NH_3								
Initial response (0-1 mm)	53	64	800	49	-27	400	13	90
High-pressure slope (5-50 mm)	2.0	4.6	12	4.2	-0.8	2.2	0.8	2.6
Acrolein	0.7	13	2.4	13	--	1.0	0.2	exponential
CO	--	--	--	--	--	0.4	--	0.2
SO_2	--	--	0.3	--	0.6	--	--	0.4
CO_2	0.2	--	1.8	0.3	--	1.4	--	--
C_2H_2	--	--	--	--	--	--	--	--

The response to ammonia is particularly interesting. Figure 19 summarizes the observed responses. There is a characteristic rise in conductance at low pressures (0-5 mm Hg), then a gradual linear rise at higher pressures (note that the entire PAPA response has been divided by 10 to get it on the same scale). The curves differ primarily in the magnitude of the initial response and in the magnitude of the slope of the linear portion. This suggests that the initial rise might be due to a surface interaction which saturates at about 5 mm Hg, while the linear portion might be due to bulk doping of the polymer film by charge transfer interaction with the gas. These data may then provide evidence for the presence of two mechanisms of gas response, and may assist in the characterization of those mechanisms. For example, both PTMP and PEP have flat responses at high pressures, but PEP has a strong initial response. A tentative interpretation of these data would be that the PEP surface conductance is enhanced by NH_3, but that the gas does not strongly affect the bulk conductivity of either polymer. PNPA, PFPA, and PPA, however, are characterized by strong linear responses but smaller initial responses, suggesting a bulk effect in these polymers but not a strong surface effect. PAPA and PEC show both strong initial and linear responses. The remaining polymer (not shown on Figure 19) is PEF. It showed a small negative response to ammonia, a result which is not well understood at this moment. Tests with PEF were not easily reproducible, and need additional work.

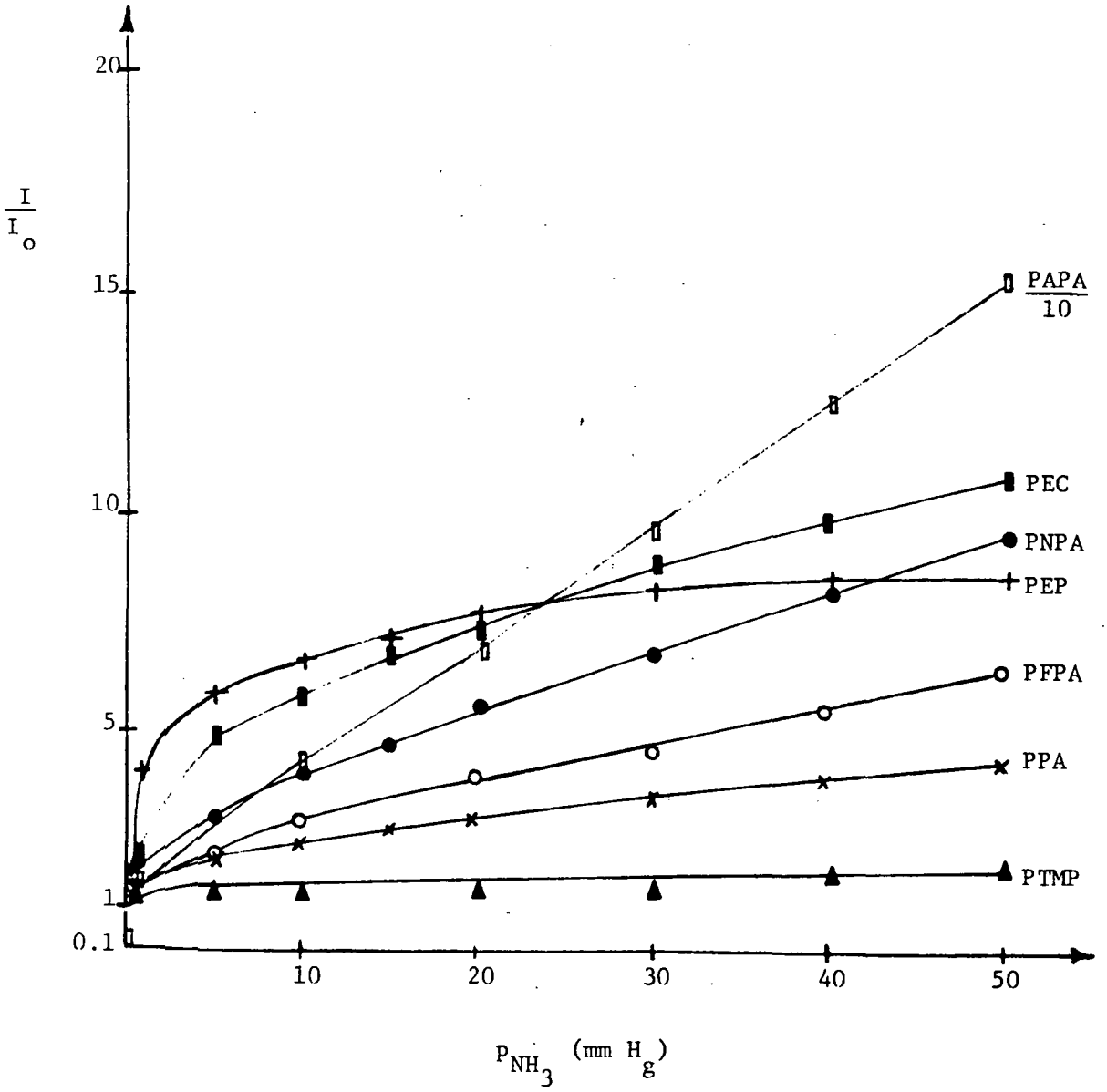

Figure 19 : Response to Ammonia

7.3 The Effect of Humidity

All polymers showed a strong response to water vapor. Typical data are summarized in Figure 20. These data were obtained in the gas-test chamber using a liquid water source from which small increments were evaporated under controlled conditions. The addition of dry air following the introduction of water vapor did not produce any effect. Four types of responses were observed. The weakest reponses were for PPA and PEF. The PPA response is shown in the figure; the data for PEF were very close to the PPA data. Stronger responses, similar to one another, were observed for PNPA, PEP , PEC, PTMP, and PAPA. Of these, four were so close to one another that the data shown for PTMP can be considered representative. The PAPA response departs from the others at higher pressures, and is distinguishable, therefore, from the other four. The PFPA response is a very strong exponential.

The data of Figure 20, which represent the responses to water vapor plus dry air under clean, controlled circumstances, do not represent the responses observed in laboratory air of corresponding relative humidities, indicating that the laboratory air contains an additional component to which the devices respond. The polymers on which this effect was most carefully studied were PNPA and PAPA. With PNPA, for example, room air of 30% RH produces an I/I_o of about 10, while the corresponding amount of pure water vapor in otherwise dry air from a commercial cylinder produces I/I_o of 4. At higher relative humidities, the effect is somewhat larger. At 80% RH in laboratory air, the PAPA devices have I/I_o on the order of 10^4,

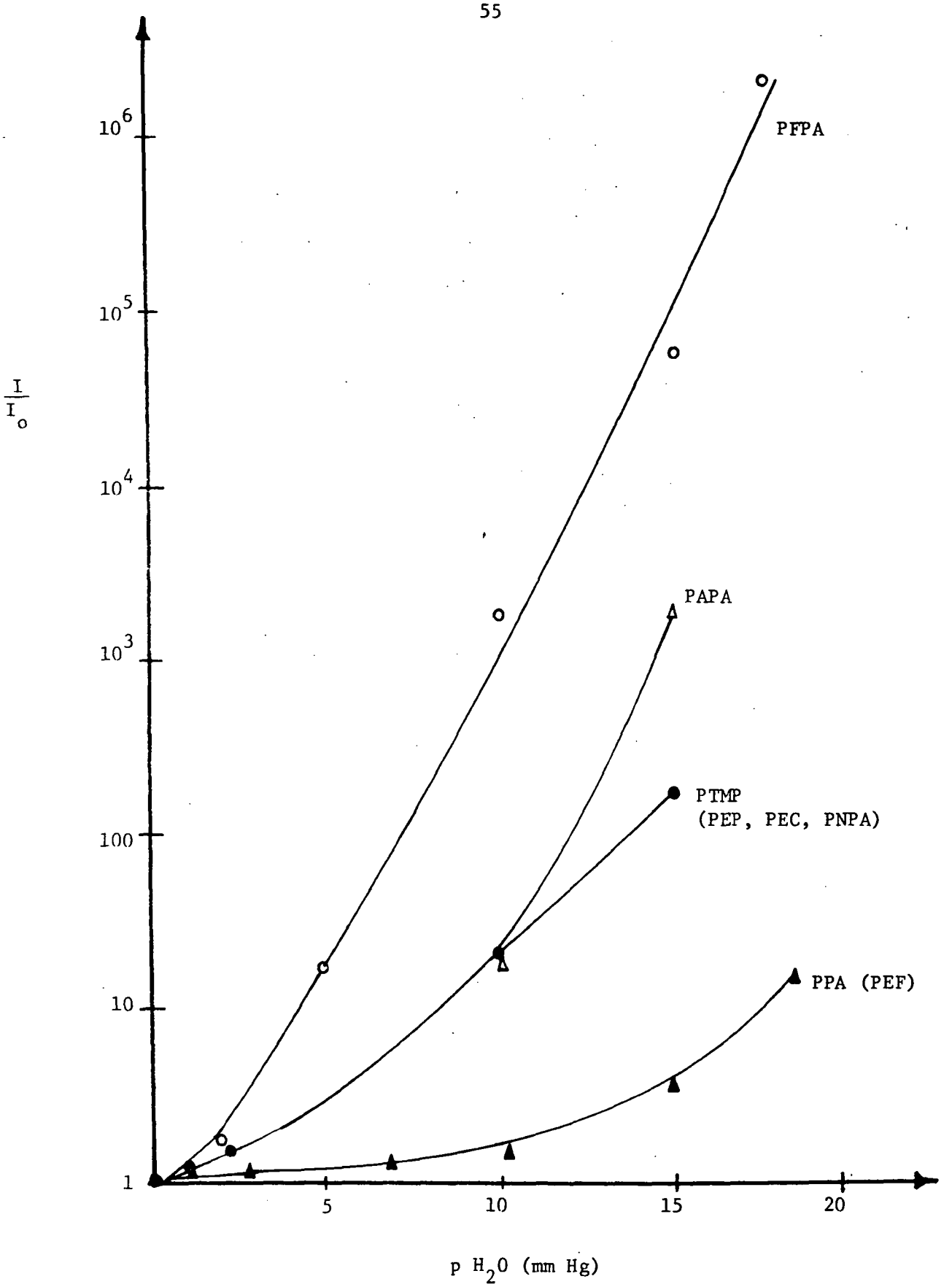

Figure 20 : Response to Water Vapor

while in the gas test chamber, the corresponding amount of water vapor produces an I/I_o value of 2×10^3.

We do not know what the component in room air is that produces this additional response. In an attempt to identify obvious candidates, we tried a number of PNPA tests with gas mixtures of water vapor plus ammonia and water vapor plus CO, CO_2, or SO_2. Only in the case of ammonia was there a strong joint response; in this case, the total response to ammonia seems to be enhanced by the presence of water vapor. Otherwise, the gas responses in the presence of water vapor were small, certainly no larger than the responses to the pure gases alone. This is an area that requires additional study.

The strong response to water vapor observed in the polymers is qualitatively similar to the effect of moisture on the surface resistivity of insulators.[9] For example, Figure 21 shows the effect of moisture on the surface resistivity of several types of glasses. At low RH, the effect is small, but above about 30% RH (corresponding to about 6-7 mm Hg in Figure 20) the surface resistivity drops sharply. There is no a priori reason to expect the surface properties of polymeric films to be highly similar to the surface properties of oxide glasses; however, there is a well-known phenomenon involving surface absorbtion of water vapor, documented in Figure 21 for glasses, that may be responsible for the polymeric responses shown in Figure 20.

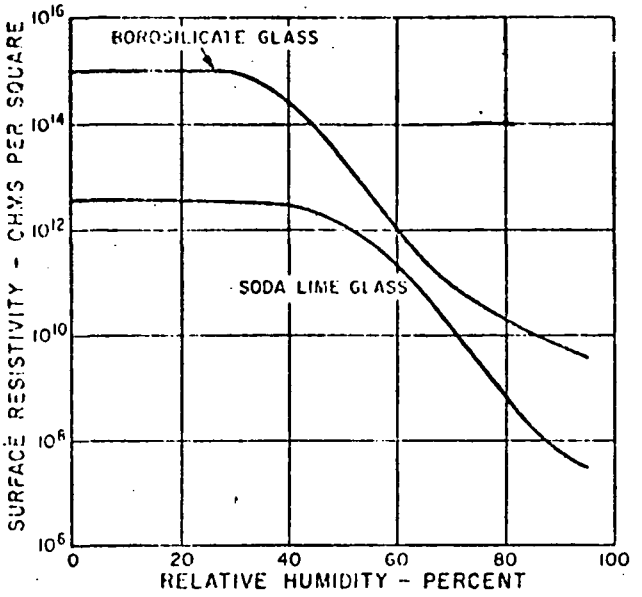

Figure 21: Effect of humidity on surface resistivity of glass (Reference 9).

CHAPTER 8 FIRE TESTS

8.1 Development of the Fire Test

In response to suggestions made at a contract progress review meeting at NASA/Lewis in January, we began the development of an incipient-fire test for our devices. This led to the construction and testing of a new chamber (Figure 22). This chamber has at one end a tungsten heater coil (1/8" i.d.) into which samples of combustible material can be inserted. At the other end is a platform on which the device under test can be placed. The device enclosure is electrically shielded to permit measurement of small currents. Air can be passed through the chamber at controlled rates. Tests have been run with dry air, room air (relative humidity in the range 28-32%), and with room air passed through a vessel containing a standard salt solution (yielding a relative humidity in the 75-80% range). The test procedure is as follows:

The chamber is wiped clean with a methanol-soaked swab to remove products of previous tests. The chamber is assembled without a device, and the leakage current between probes measured (to insure that stray current paths do not contribute to test results). A charge is then placed in the heater coil and the device is installed. Air of the appropriate relative humidity is flowed through the chamber. The current through device with 50 volts applied is monitored. When device current reaches a stable value (usually within a few minutes), the heater is turned on. The heater current has been set at a level so that there is no flame or visible glowing of

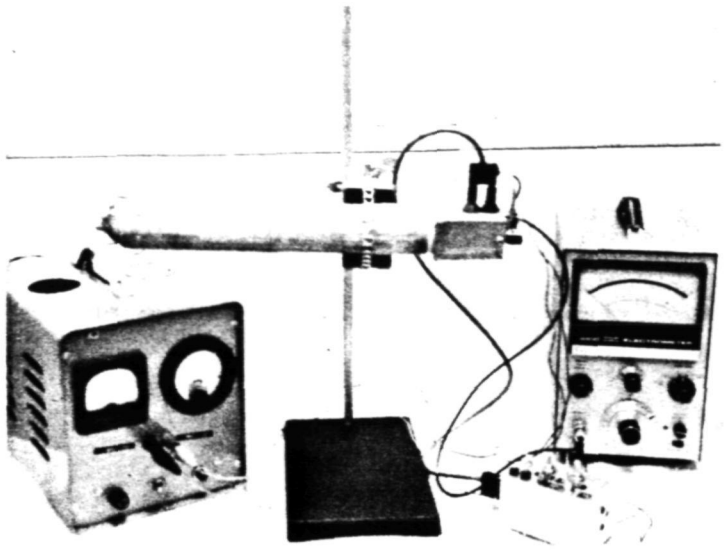

a) Fully assembled

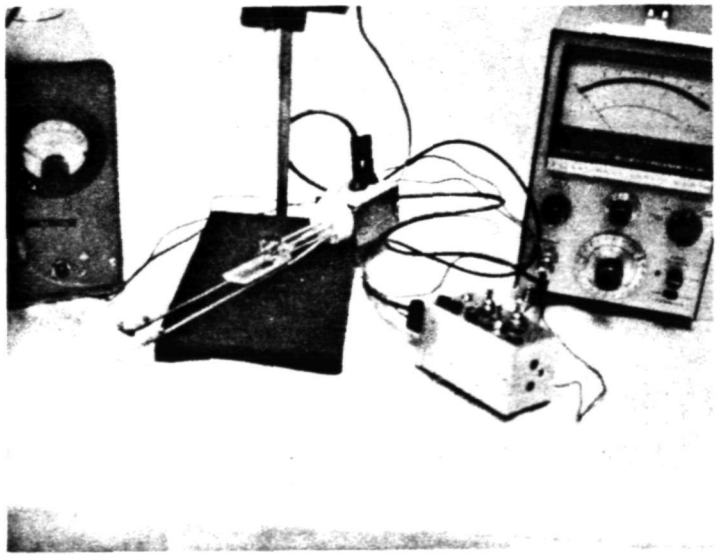

b) Dissembled, showing tungsten filament (left) and device platform (right).

FIGURE 22: FIRE-TEST CHAMBER

the charge, but so that visible smouldering begins to appear about 40 seconds after heater turn-on. With the charges used, 6 mg of cotton thread, smouldering persists until about 130 seconds after turn-on. With the selected standard heater current (2.6 amperes), 3.5 mg of the cotton is consumed during a test cycle. The residue is charred, but the threads are physically intact.

A critical parameter in the test is the air-flow rate. If there is no air flow, combustion products will build up in the chamber producing concentrations which may be unrealistically large for an incipient fire. If the air flow is too large, combustion products are swept from the chamber too quickly to interact with the sensor. The volume of the chamber is 380 cm^3. Figure 23 shows two graphs of response amplitude versus flow rate for PAPA lock-and-key devices. The definition of response amplitude is discussed more fully below. For the present, it is sufficient to consider how this parameter varies with flow rate. At low flow rates, below 1000 ml/min, there is observable build-up of visible smoke within the chamber. There is also, as Figure 23 shows, substantial increase in apparent device sensitivity. Because the device response is so strongly dependent in flow rate in this low range, we decided to operate our tests at a higher flow rate of 1740 ml/min, indicated by the arrow in Figure 23, at which the device response is relatively independent of flow rate. By choosing a value in this range, we believe we are providing conditions that more realistically approach the incipient fire than would stagnant conditions in a small volume. At the flow rate of 1740 ml/min and with a 6 mg

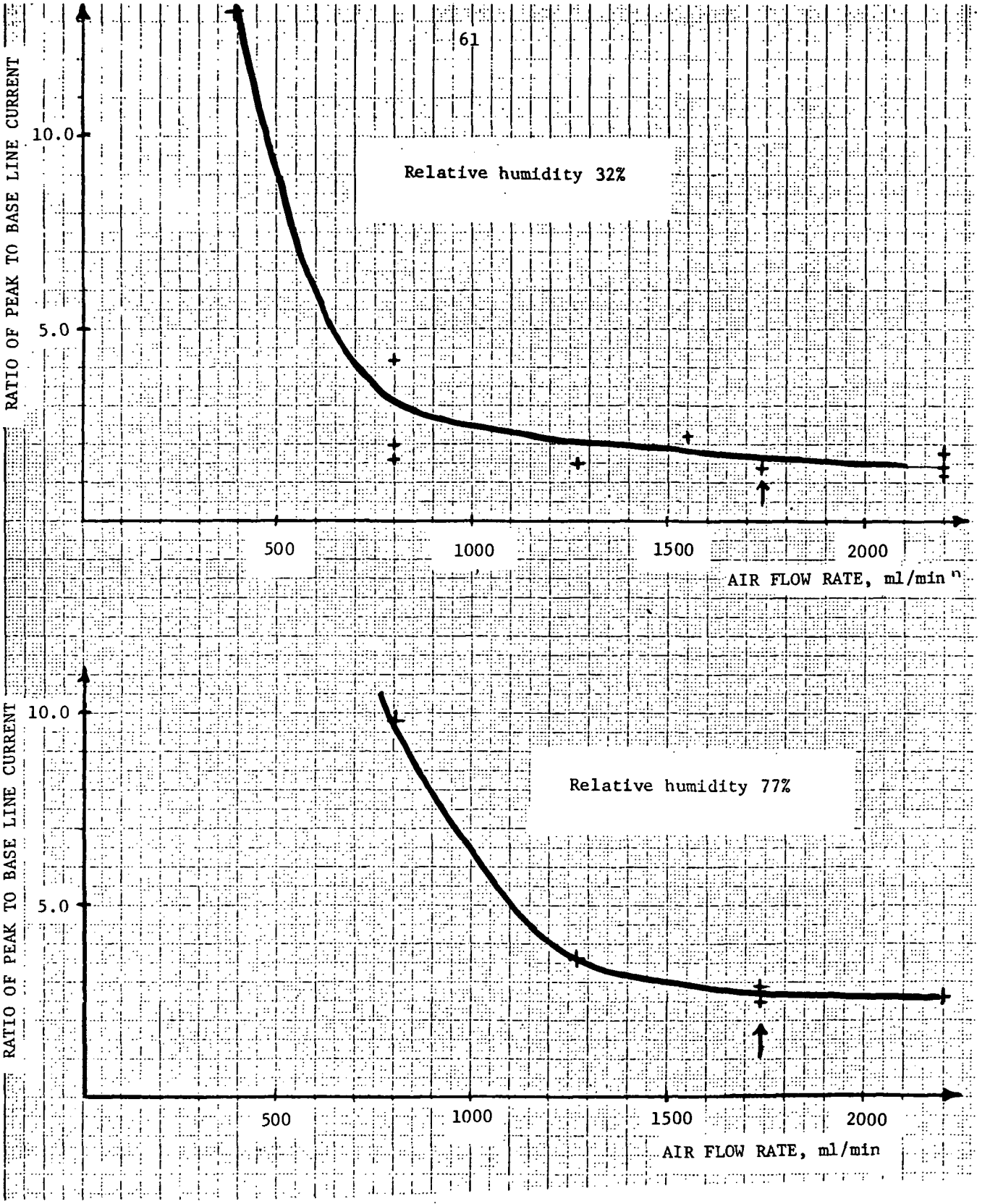

Figure 23: Dependence of fire-test response on air-flow rate. The arrow denotes the value selected for standard tests.

charge, it is not possible to observe visible smoke building up within the chamber. Nevertheless, as the data show, the devices do respond. Since an incipient fire detector should be capable of responding before the density of combustion products reaches the level of visible smoke, we feel that our test, which yields smaller responses than a stagnant test, is a reasonable first approximation to reproducible incipient-fire conditions.

8.2 Test Results

Fire tests have been run with all eight polymers. A typical test is shown in Figure 24, illustrating the response with a device coated with PAPA. There is a small peak twenty seconds after turn-on (which may be from moisture evaporated from the charge) and a larger peak at about one minute after turn-on. Heater power is not turned off until after the response passes through a peak. The device recovers fully within minutes. For the test shown, the ratio of peak response (I_{max}) to device current before turn-on (I_0) is 2.65. Proof that the device is responding to combustion products rather than heat is obtained by repeating the test without a charge. No response is observed without a combustible charge in the heater coil.

Tests show that a freshly prepared device must undergo a break-in or aging process (during which the baseline current I_0 drops by as much as an order of magnitude) before it yields reproducible test results, but that after three or four tests, most devices are quite reproducible. One device coated with PAPA has been used for over twenty-five fire tests and still responds well and predictably to the test fire.

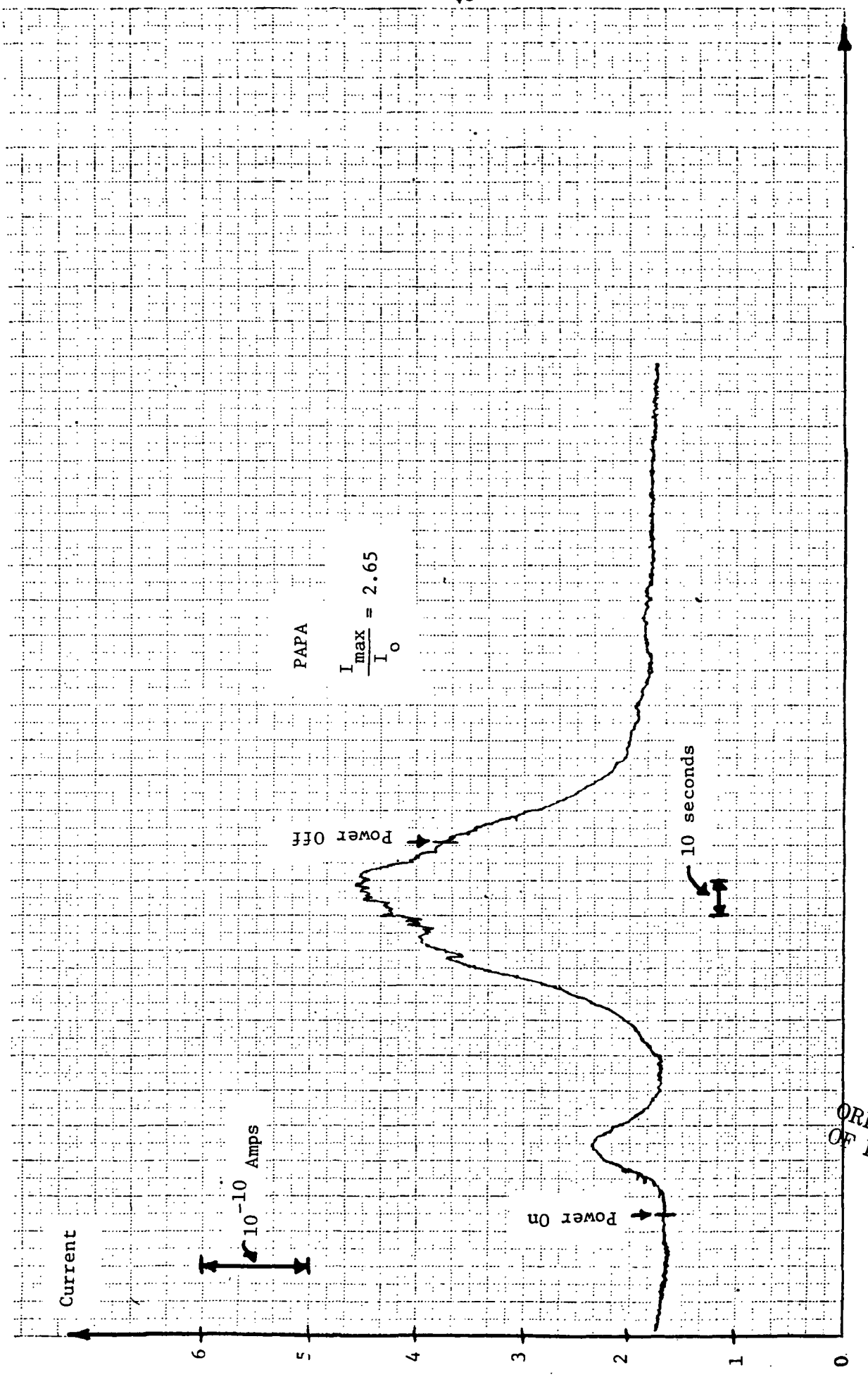

Figure 24 : Fire-test of a lock-and-key device coated with PAPA

The differences between polymer responses are primarily in the peak height of the response during the test fire. Figures 25 and 26 show typical traces for PNPA and PPA. Table V summarizes the test data for all polymers at 30% relative humidity. The excellent responses of PTMP and PEP (which were received too late in the contract to permit their inclusion in the program of long-term tests) suggest that further investigations should be made with these particular polymers. The huge PEC response may be deceptive. There is question whether the polymer actually is poly(ethynyl carborane) based on spectroscopic and thermogravimetric analysis;[6] our experience is that devices coated with PEC behave almost like an uncoated electrode (see below).

In order to test whether the response was a surface effect, we tested an uncoated electrode in the fire chamber. The I_0 for the uncoated electrode is critically sensitive to the cleanliness of the surface. Figure 27 shows a fire test on a cleaned uncoated electrode, tested in laboratory air at 29% relative humidity. The apparent sensitivity, using the ratio of I_{max} to I_0 as a parameter, is enormous. The ratio is 18.4. However, it is interesting to compare the magnitudes of I_{max} for the PAPA test (Figure 24) and the uncoated electrode test (Figure 27). They are within 20% of one another. This strongly suggests that a surface effect is contributing to the response. Data presented in Chapter 9 will document that a bulk effect is also present.

One should not conclude because the fire response is partly a surface effect, that the polymer is useless. In contrast to the polymer

TABLE V

SUMMARY OF FIRE TEST DATA

POLYMER*	I_{max}/I_o at RH $\approx$ 30%
PPA	1.0
PNPA	1.4
PAPA	2.7
PFPA	2.7
PEF	2
PTMP	7
PEC	20
PEP	7

* All devices made from 4% solutions

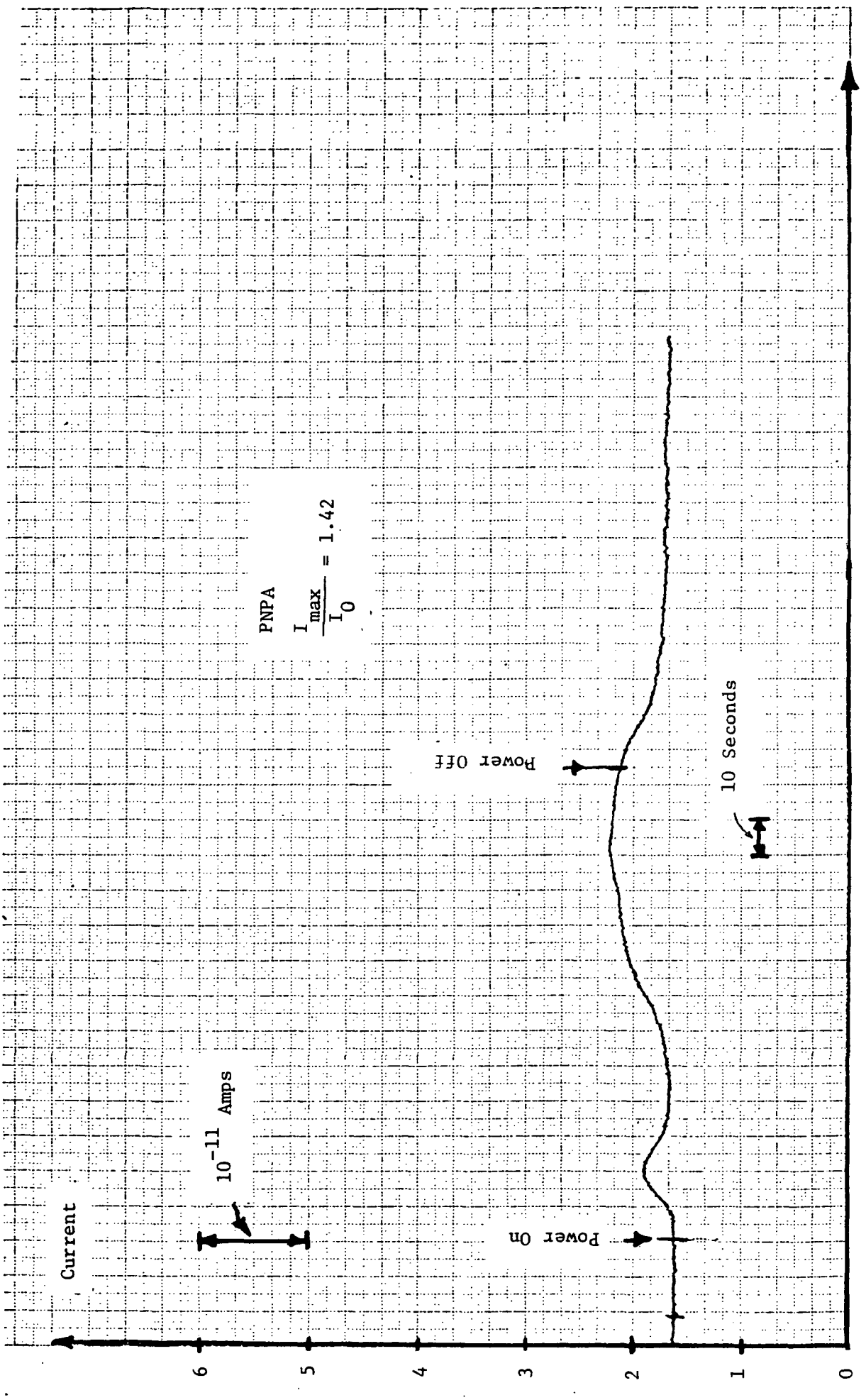

Figure 25: Fire-test of a lock-and-key device coated with PNPA

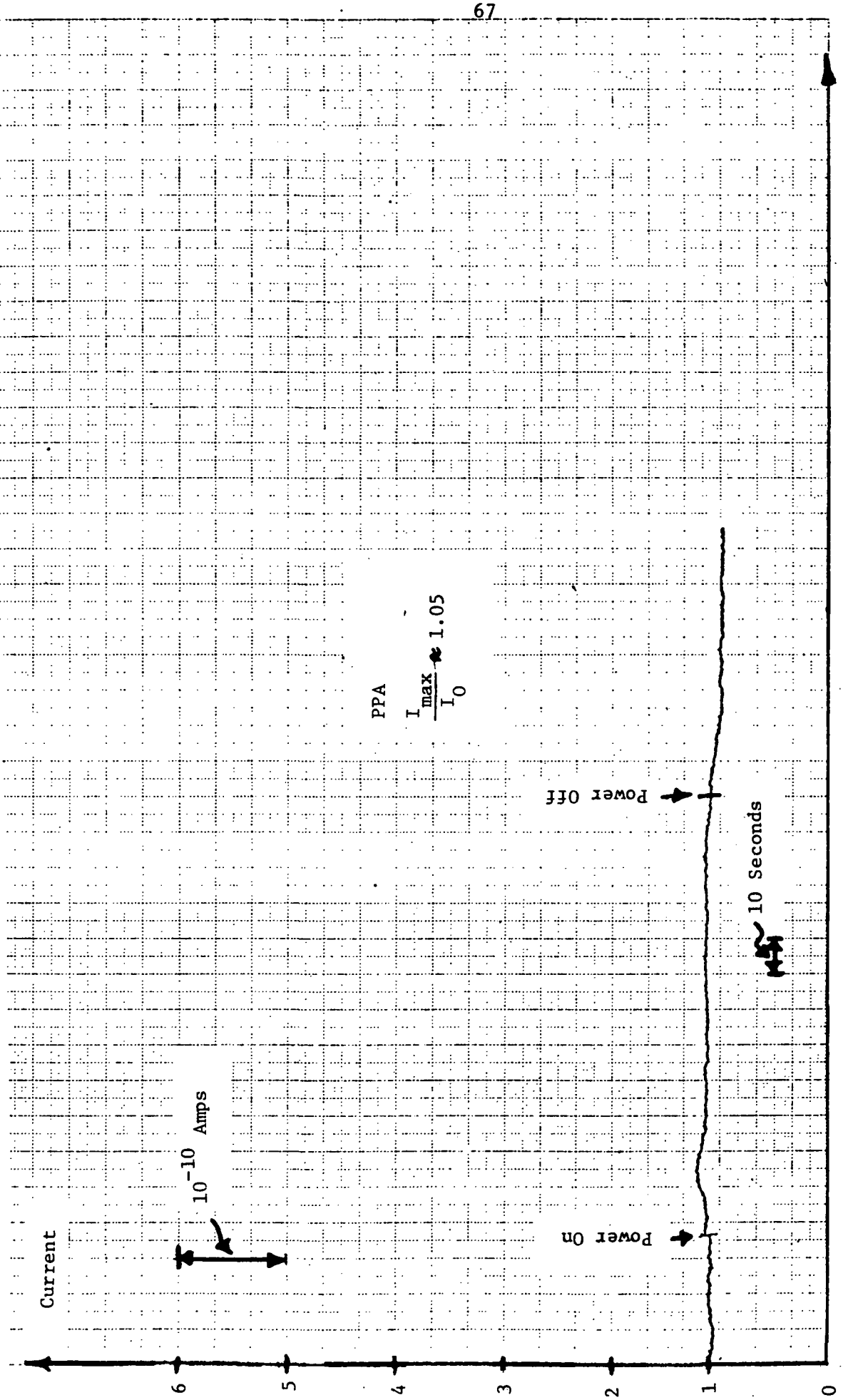

Figure 26 Fire-test of a lock-and-key device coated with PPA.

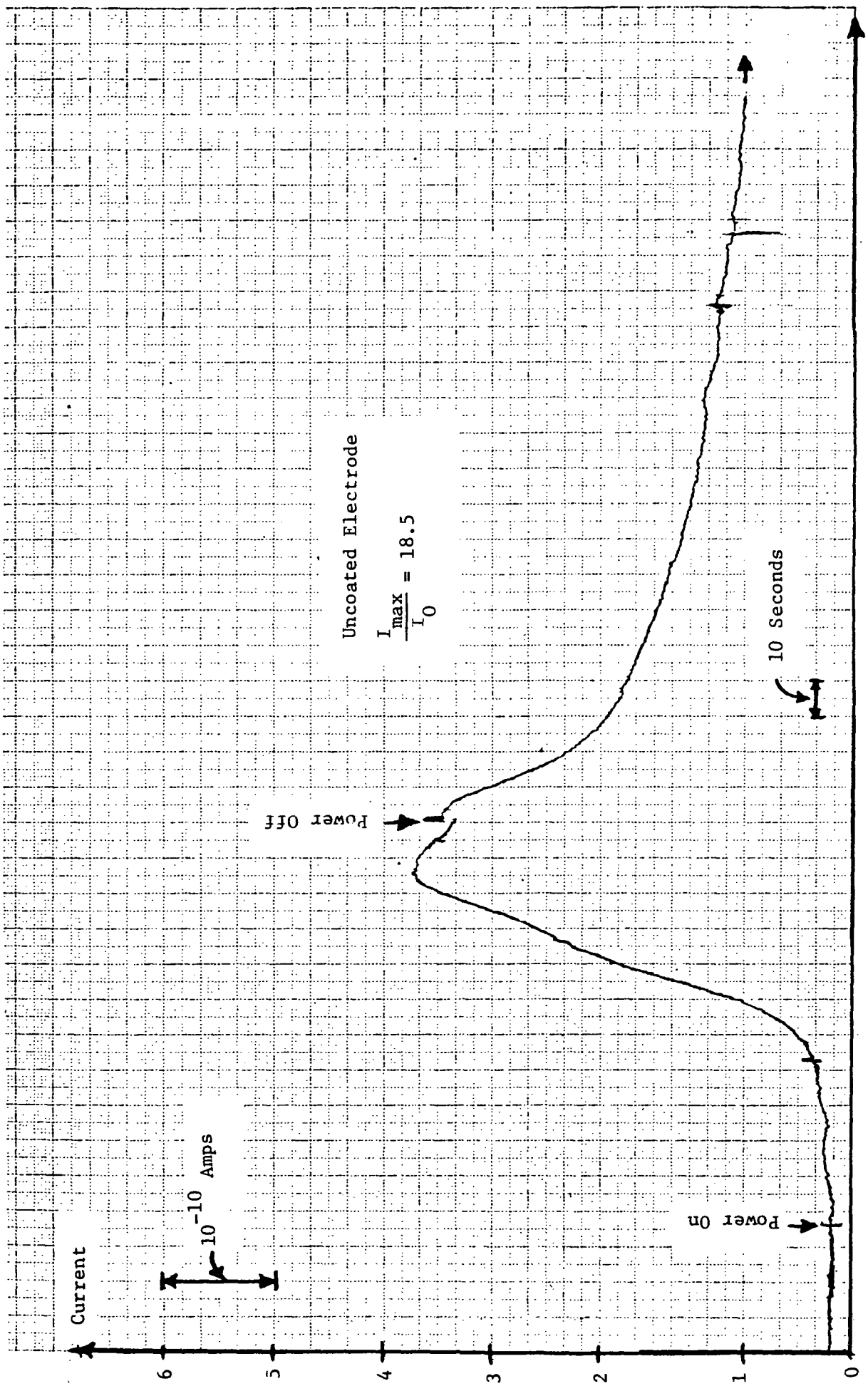

Figure 27: Fire-test of a cleaned, uncoated lock-and key electrode.

devices, the uncoated electrode is extremely variable in its response, being unstable and non-reproducible. The polymer devices, however, are quite reproducible and can be cycled through the test many times with comparable results. There is in addition, an interesting correlation between the peak amplitude of response and apparent dielectric constant based on our thin-film sandwich data. The materials with the highest dielectric constants show the strongest responses.

In the case of PAPA, we have examined the effect of humidity on device performance. Figure 28 shows the variation in the background conductance (lower curve) with relative humidity at room temperature, and the corresponding variation in the peak conductance in the presence of combustion (upper curve). These results show that although the background current is a strong (exponential) function of relative humidity, the ratio of peak response to background response is relatively independent of humidity. This will permit the identification of a stable threshold alarm level provided that the humidity dependence of the background can be compensated.

Corresponding humidity-dependence data for an uncoated lock-and-key electrode are shown in Figure 29. The fire response is similar in magnitude or larger than that of the PAPA devices, but the data reproducibility is quite poor. The polymer-coated devices, however, combine adequate sensitivity with good reproducibility.

Figure 28: Variation in the background current (lower curve) and peak response to a 6 mg cotton incipient fire (upper curve) for a lock-and-key device (no. 1-3-2) coated with PAPA [poly(p-aminophenylacetylene)], based on 9 tests at 22-23°C.

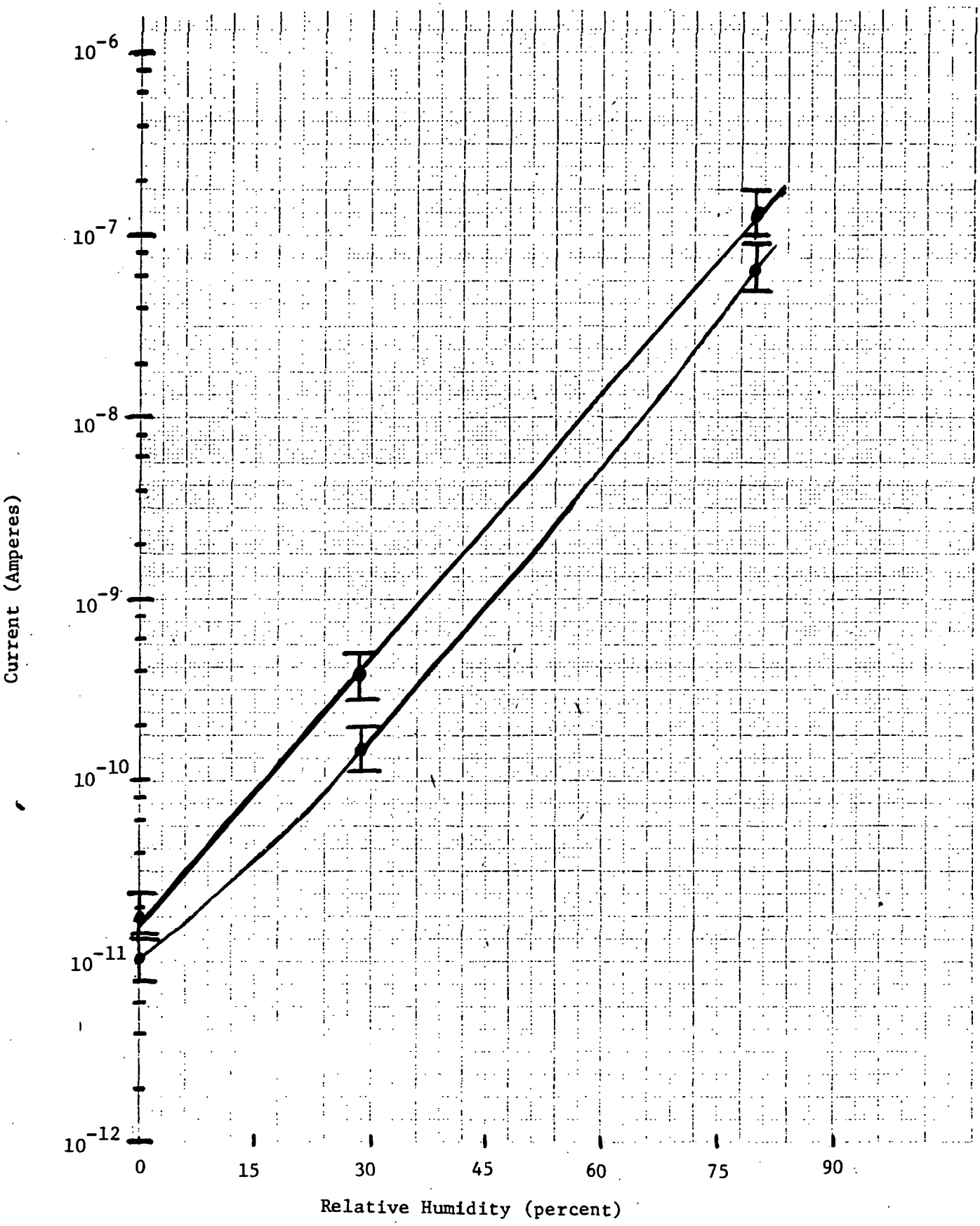

Figure 29: Variation in the background current (lower curve) and peak response to a 6 mg cotton incipient fire (upper curve) for an uncoated lock-and-key device (no. 1-3-5) based on 16 tests at 22-23°C.

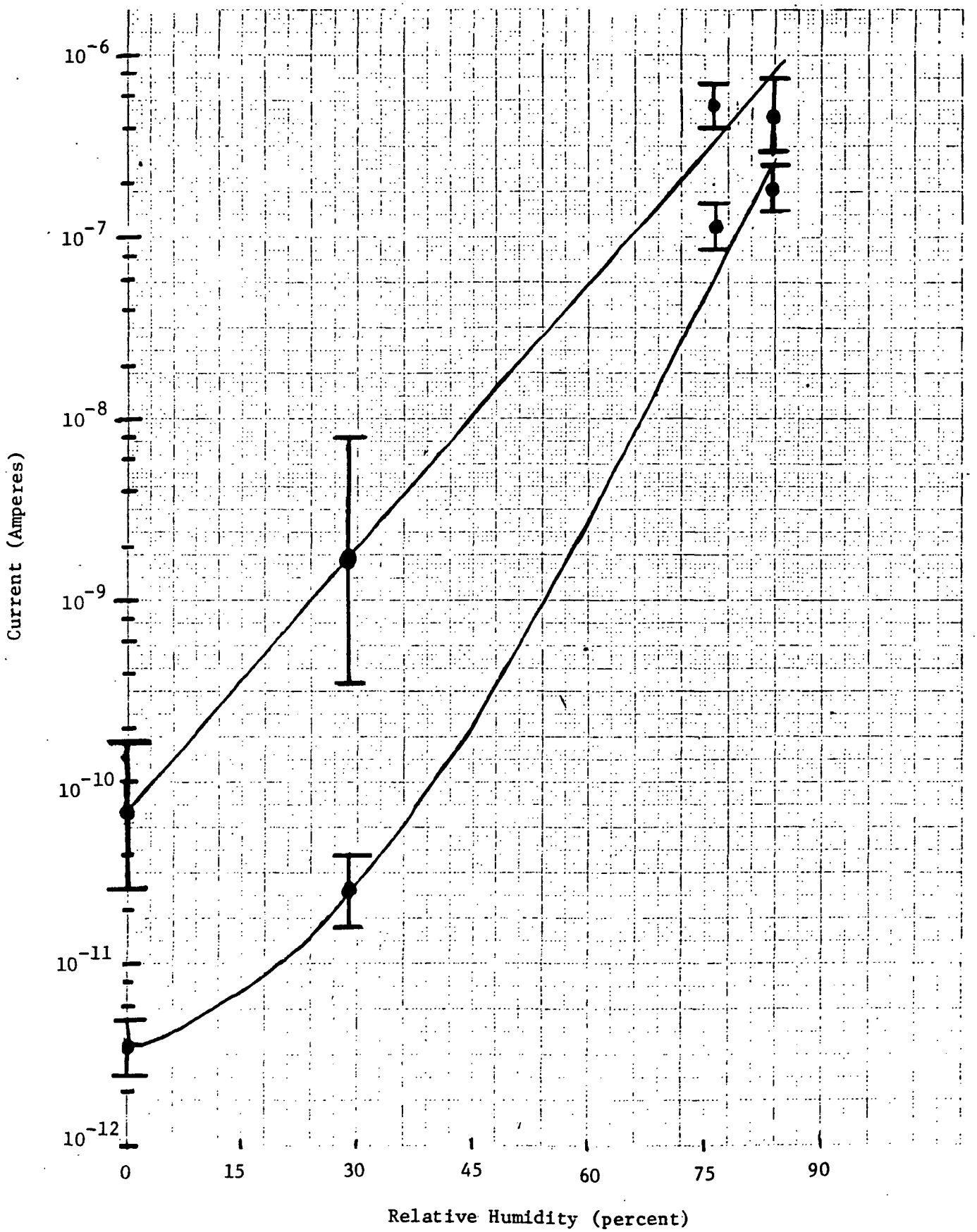

CHAPTER 9 LONG-TERM TESTS

9.1 Selection of Polymer and Device Configuration

The purpose of the long term tests was to determine the reproducibility and aging characteristics of devices, including possible effects of contaminants present in normal ambients, and the effects of exposure to temperature variations and to light. Within the limited space of a one-year contract, the time available for such tests was obviously limited. Furthermore, selection of device configuration and polymer had to be concluded before the receipt of all polymers. Thus the tests reported here are indicative of what can be expected from other devices and polymers, but do not necessarily represent the best device-polymer combination that can be made with present technology.

The decisions on device configuration and polymer selection were made in June, 1974. The lock-and-key device configuration and the poly (p-aminophenylacetylene) polymer were selected on the basis of recorded responses in the gas-test chamber and in the fire tests. The formamido polymer (PFPA) was also considered, but was rejected because it seemed to have a slightly slower response than PAPA, and it was more susceptible to ill effects from device processing.

9.2 Test Devices

A set of forty new lock-and-key substrates were made. Each one was tested in vacuum for conductance prior to coating. Most devices showed

leakage currents in vacuum of between 3.5 and 4.3 x 10^{-12} amps with 50 volts applied, corresponding to device conductances of about 0.8 x 10^{-13} mhos, in excellent agreement with theoretical expectations. Devices with leakage currents greater than 4.5 x 10^{-12} amps were rejected. In all, twenty-five substrates were selected from the original set of forty.

The set of twenty-five devices was used to test the effect of five different environments, and to test whether variations would be observed from polymer solutions of differing concentrations and differing ages. Five groups of five devices each were formed. All the members within a group of five were coated from the same polymer solution using identical procedures. The five solutions used are described in Table VI All were filtered just prior to application. Examination of the devices under a microscope showed that all coatings were of good quality.

Immediately after coating, all devices were tested for <u>in vacuuo</u> conductance, and for conductance in one atmosphere of clean, dry air. In vacuum, all devices exhibited a transient decrease in current after initial turn-on, with a time constant on the order of minutes. After completion of this transient, the <u>in vacuuo</u> leakage current was in the range 3.5 to 4.3 x 10^{-12} amps, unchanged from the result with uncoated electrodes. In one atmosphere of dry air, this current increased slightly, to a range of 3.7 to 5.3 x 10^{-12} amps. The average increase was 0.44 x 10^{-12} amps between vacuum and one atmosphere of clean dry air, an increase in conductance of about 10%.

TABLE VI

POLYMER SOLUTIONS FOR LONG-TERM TESTS

A	4% PAPA	first prepared in November 1973
B	10% PAPA	prepared fresh in June 1974
C	10% PAPA	prepared in April 1974
D	4% PAPA	prepared in April 1974
E	4% PAPA	prepared fresh in June 1974

9.3 Performance of New Devices

One device from each polymer-solution group was selected for fire testing prior to placing the devices in various environments. This subset of five devices thus established a standard of performance to which devices could be compared after exposure to differing environments. The devices were tested four or five times in the fire-test chamber. After the first two tests, the device baseline current (I_0) usually settled down to a reproducible value, and the fire tests yielded reproducible results thereafter.

The response of these devices is summarized in Table VIII (page 79). Note the very important result that the devices coated with 10% solution were significantly more sensitive than the devices coated with 4% solution, in fact, 2.5 times more sensitive. This result argues strongly for the presence of a bulk effect in the response of these devices, because polymer thickness is roughly proportional to solution concentration. This result also shows that the response observed is not due to the glass surface, because the glass surface is better isolated from ambient with a 10% coating than with a 4% coating, yet the 10% devices respond better.

A tempting model is that both the polymer surface and the polymer bulk are contributing to the device response, and that the role of the glass surface is to provide a background current which ultimately limits the sensitivity. Future work should concentrate on unraveling these three contributions to device behavior.

9.4 Exposure to Test Environments

The five groups of five devices, each group coated with a different polymer solution were then regrouped into five new groups, with each new group containing one device from each solution. Each of these new groups of devices was placed in a selected environment for about one month. The environments were a kitchen, an office, a dark dry-box, a refrigerator and outdoors. More explicit details are contained in Table VII.

The devices had no voltage applied during this one month test, so that the test does not correspond to operating conditions. However, the test environments should provide insight into possible contaminant effects and to the effects of sunlight.

After exposure for one month, the devices were examined under a microscope. They were then tested in the fire-test chamber. The characteristics of the 4% devices were widely varied and unpredictable after exposure. The ratio of peak current to background current varied from 1.9 to 19, with no discernible correlations from environment to environment or from solution to solution. One device, from the oldest solution and exposed to the kitchen environment, did not recover after the second fire test, and behaved virtually like an uncoated electrode (with a response ratio of almost 20). All other 4% devices responded, with a mean ratio of 7 and a standard deviation of 6.3.

The 10% devices behaved much more consistently as a group. Two devices had baseline currents which kept drifting. One of these was coated with the fresh 10% solution, and was exposed outdoors; the other was

coated with the older 10% solution and was kept in the refrigerator. The other eight devices responded quite consistently, with a response ratio of about 2 (the mean was 2, the standard deviation 0.7). Thus two devices failed and the others as a group showed a decrease in sensitivity from the baseline value before exposure.

With the exception of the correlation with solution concentration, no other significant correlations could be obtained from the test data. Age of solution and environment had no systematic effect on device performance.

TABLE VII

DESCRIPTIONS OF TEST ENVIRONMENTS

1. Kitchen. (July 10 - August 6, 1974) Devices were placed in the kitchen of an MIT fraternity house. The kitchen is large, ventilated, is used by about 20 persons, and contains one oven, a grill, and 4 gas burners. The devices were placed near the ceiling on a wall about 20 feet from the stove. The oven, burners and grill were all located beneath a fan hood. Devices left in this environment were found to have patches of dust and dirt adhering to their surfaces after exposure, but were otherwise in excellent condition.

2. Office. (July 14 - August 12, 1974). Devices were placed on a shelf in an office where they were exposed to direct sunlight for several hours per day. The office was air-conditioned, with temperatures in the 70 - 80° range and relative humidities in the 40 - 60% range. The devices appeared to have faded after exposure; the coating looked lighter as if bleached by the sun.

3. Dry box. (July 10 - August 5, 1974). Devices were placed in a nitrogen dry-box covered with aluminum foil to exclude light. Except for the foil covering, this was identical to the storage method used for all devices when not being tested.

4. Refrigerator. (July 10 - August 8, 1974). Devices were placed in a laboratory refrigerator maintained at about 37°F. The inside of the refrigerator was dark and humid; moisture condensed on several devices. After exposure, one device had dust on it; the others were unharmed.

5. Outdoors. (July 11 - August 9, 1974). Devices were placed outside but sheltered under an eave so that they were not exposed to direct sunlight or to rain. After exposure, the devices showed dirt adhering to the surface, but no other ill effects.

TABLE VIII

RESULTS OF LONG-TERM TESTS

Average Response Ratio

	4%	10%	ALL
Standard	1.9 ± 0.3 (3 devices)	5.2 ± 2 (2 devices)	3.3 (5 devices)
After exposure	7 ± 6.3 (14 devices)	2 ± 0.7 (8 devices)	5 (22 devices)

CHAPTER 10 DEMONSTRATION SYSTEM

10.1 Design and Construction of a Demonstration System

A demonstration system which includes a lock-and-key device coated with one of several different polymers, measurement circuitry, an alarm threshold circuit, and an audible alarm was designed and built for the purpose of illustrating device operation under normal ambients. The demonstration system consists of three parts (see Figure 30), a sensor/battery pack (which includes a 50-volt battery in series with a sensor), a current amplifier (the Keithley picoammeter), and a detector/alarm unit which was custom built in our laboratory.

The sensor/battery pack has a screened shield to provide electrical isolation while permitting combustion products to reach the device. At present, the flow of gases through the screen is less than ideal, and future designs should address more carefully the air-flow characteristics of the enclosure. The sensor/battery pack does however provide a relatively, compact way to package the device. A single cable leads to the picoammeter, and a single cable leads from the picoammeter output to the detector/alarm unit.

The decision to use a commercial current amplifier was made in order to save engineering time and costs at a point in the program where final design parameters were not yet specified. Ultimately, the picoammeter is to be replaced by a field-effect-transistor amplifier,with specified gain and impedance parameters which could be incorporated into the sensor/-

a) Assembled system, showing the sensor/battery pack in the foreground, the commercial picoammeter used as an amplifier, and the detector/alarm unit.

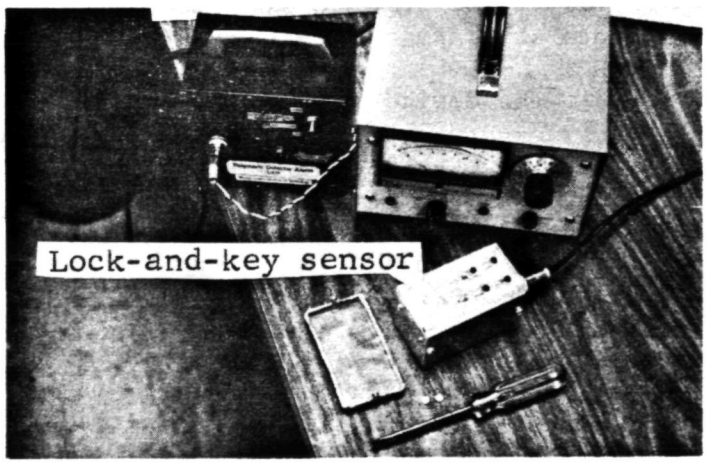

b) Top view, with screen removed from sensor unit.

Figure 30: Polymeric Detector Demonstration Unit

battery pack. The variability of the devices now under test favor the flexibility of a multi-range commercial instrument for routine use.

The circuit for the detection/alarm unit is shown in Figure 31. It operates from its own batteries. In the OFF possition, the batteries are disconnected. In the BATT TEST position, the batteries are connected across a pair of light-emitting diodes. If the batteries are good, both lights are on. In the SET position, the potentiometer is adjusted until the indicator light is on the verge of lighting. This adjustment represents the compensation for the humidity variation of the background current of the device under test. Normally, once this threshold is set, no further adjustments are required provided that the ambient does not change significantly. Finally, in the ARM position, the threshold detector is armed, and will indicate an alarm condition with both indicator light and audible alarm whenever the device current exceeds the threshold level. In the present design, the threshold level is 1.5 times the background current. This threshold level can be easily changed as needed.

The demonstration system has been used in conjunction with various volatile liquids, with smouldering cotton swabs, burning cigarettes, and with actively flaming matches. Of the volatile liquids, only water provides a significant response. Acetone, methanol, and other solvents do not set off the alarm. Smouldering swabs and burning cigarettes produce an alarm provided that the air currents do not carry the combustion products away from the screened sensor. An actively burning match, which provides not only combustion products but also a convection current to drive

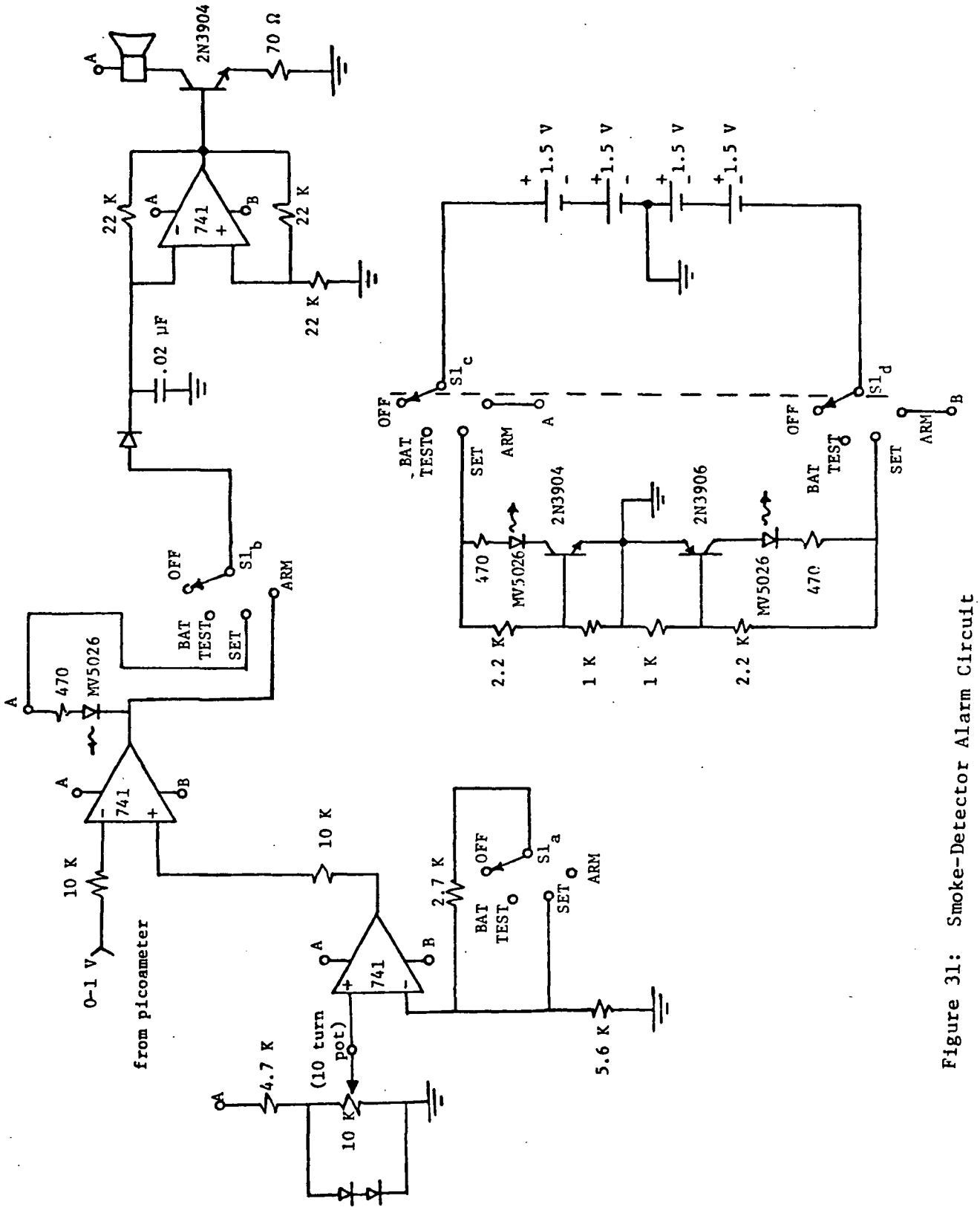

Figure 31: Smoke-Detector Alarm Circuit

those combustion products through the screen, produces a rapid response. When the source of response is removed, the current returns to its background level.

The demonstration system has been exhibited in a Contract Review meeting held at NASA Headquarters in Washington, DC on October 16, 1974.

10.2 Results

Based on the experience we have had with the demonstration unit, we conclude that it is possible to build a polymeric fire detector that responds to the emanations of smouldering and active fires, and that this polymeric detector has advantages (such as requiring no heater, and not responding to common organic solvents) not presently available in the widely discussed Taguchi Gas Sensor based on semiconducting stannic oxide. Thus the polymeric approach continues to be an attractive route to a low-cost early-warning fire detector.

CHAPTER 11 DISCUSSION

It is appropriate to conclude this technical report with a discussion, in broad perspective, of the goals of this effort, of the degree to which those goals have been met, and of those aspects of the program which should receive additional attention in the future.

The most fundamental question addressed in this program has been whether it is feasible to use polymeric sensing devices to build an early-warning fire detection device. This program has indeed demonstrated that polymeric sensing devices are capable of responding to the emanations of smouldering and actively burning fires. The principal interfering species is moisture, and efforts are needed to develop a compensation method for these devices.

We have furthermore shown, in agreement with other work,[6] that each polymer has its own profile of responses to gases and to combustion products, and that suitable combinations of polymers may yield significant improvements in discrimination between hazardous and non-hazardous ambients.

We have developed a quantitative model of device performance with which many of our results can be understood. This model has helped identify the role of the polymer bulk properties in overall device performance, and has pointed to substrate surface effects and polymer surface effects as significant components. The model suggests further that observed responses to gases may be combinations of bulk and surface responses which may be unraveled by new experiments in which the thickness

of the polymer film is treated as a variable.

Conclusions based on this model point to the desirability of finding new polymeric materials with higher in vacuuo conductivities but with relative responses comparable to existing polymers. This does not rule out, however, the possibility that one of the polymers already available, or that a combination of polymers already available, might be capable of producing a fully satisfactory alarm unit.

Ultimately, we look to miniaturization as a way of improving performance and reducing costs. In this regard, a device design developed by Wishneusky at MIT, is most attractive. The device, first described in Wishneusky's thesis,[5] is illustrated in Figure 32.

A finger electrode is deposited on a substrate (silicon or glass). Then a thin insulator is applied over this electrode. This insulator can be made of silicon dioxide, and can be either sputtered or spun onto the lower electrode. A second electrode is then applied above the insulator, but with the fingers staggered so that the metal fingers in the upper electrode are over the spaces in the lower electrode. The polymer film is then applied over this upper electrode.

Device operation is as follows. When the polymer is insulating, the interelectrode capacitance is very small. When the polymer film becomes conducting, whether through a bulk or surface effect, the interelectrode capacitance increases dramatically. What is measured is the waveform of the charging current of the interelectrode capacitance when the device is subjected to a voltage step. The magnitude and duration

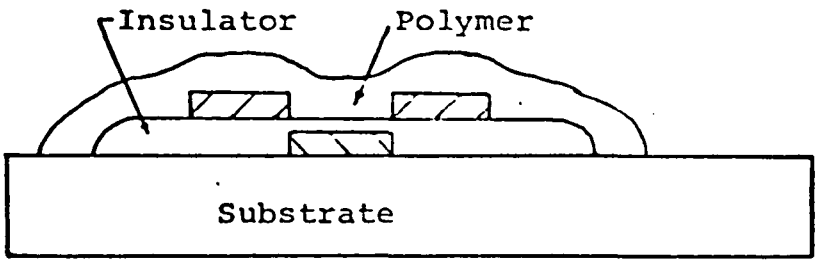

Cross-Section View

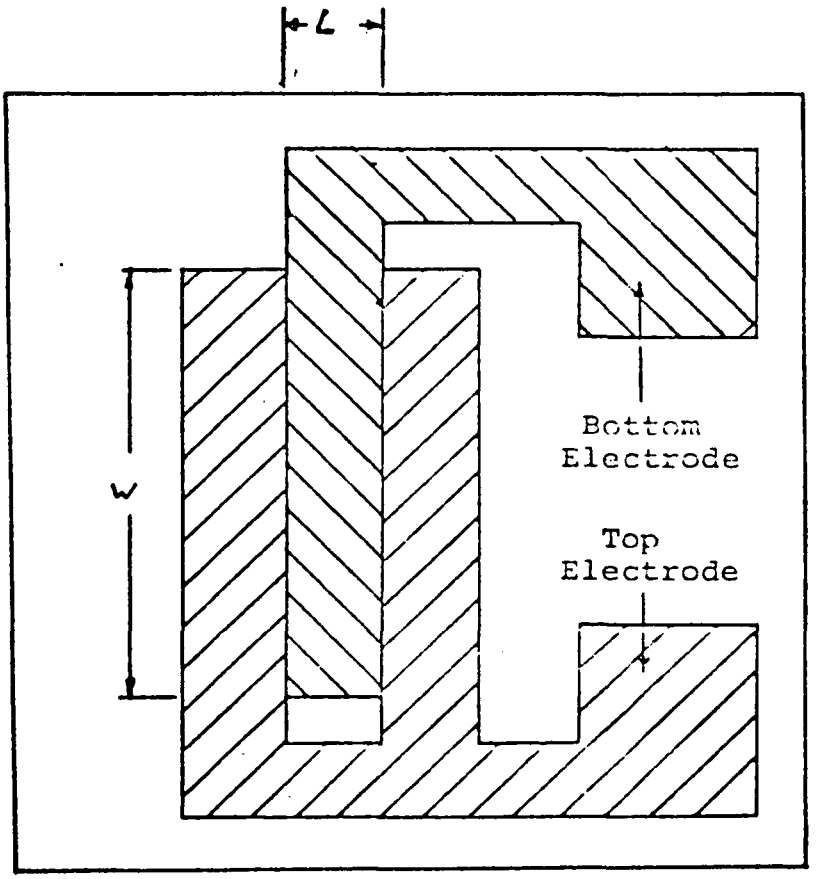

Top View

Figure 32: Schematic of Wishneusky device (Reference 5).

of the charging current will increase when the polymer film becomes conducting.

The advantages of the Wishneusky device configuration over all others are these:

1. Processing: The polymer is applied last. Thus the entire wafer processing, including the fabrication of detection and alarm circuits elsewhere on an integrated circuit chip, can be done prior to the application of the polymer.

2. MOS compatibility: Because the device responds to a voltage step, it can be introduced immediately into MOS integrated circuits without any special interfacing.

3. Miniaturizability: This device, although originally conceived as a large-area device, can be miniaturized and can become part of an integrated sensor/detection circuit package.

4. Economy of size and cost: A field-effect device based on the Wishneusky principle can be used to combine sensing and detection functions in a single integrated device. This one device would replace the sensor, the current amplifier, and the detector circuit of the present demonstration system.

In view of the above discussion, we strongly recommend that further work be done on the polymeric sensors, and that this work be directed towards several specific goals:

1. The extensions of our knowledge of the properties of existing polymers, including the separation of bulk and surface effects in the responses.
2. The development of multi-element sensors which compensate for humidity and which take advantage of the different response profiles of different polymers.
3. The fabrication and testing of devices based on Wishneusky's design, as the most promising route toward an integrated, low cost, polymeric fire detection device.

New polymers should also be explored, as they become available. It is clear, though, that the properties of existing polymers have not yet been fully exploited.

REFERENCES

1. N.R. Byrd, "Space Cabin Atmosphere Contaminant Detection Techniques", Douglas Report SM-48446-F, Contract NAS 21-15, July 1968.

2. See for example, M.M. Labes, J. Polymer Science, Part C, no. 17, pp. 95-105 (1967).

3. D.J. MacFadyen, 1973 Annual Report NASw-2022, Abt Associates Inc. #73180, Dec. 1973.

4. K.W. Kawate, "The Spectra of Polyphenylacetylene", S.M. and E.E. Thesis, MIT, June 1974.

5. J.A. Wishneusky, "Device Structures for Microelectronic Gas Sensors", S.M. and E.E. Thesis, MIT, Sept. 1974.

6. N.R. Byrd and M.B. Sheratte, "Synthesis and Evaluation of Polymers for use in Early Warning Fire Alarm Devices", McDonnell Douglas Corp., NASA CR-134693, 1975.

7. T. Kaplan and D. Adler, Applied Physics Letters, 19 418 (1971).

8. F.M. Clark, Insulating Materials for Design and Engineering Practice (New York, Wiley, 1962) pp. 997-1000.

9. Ibid., p. 998.

APPENDIX A

ADMITTANCE OF LOCK-AND-KEY DEVICES

This Appendix contains the derivation of the expression for the admittance of lock-and-key devices used as the basis for interpretation of electrical, gas-test, and fire-test measurements. The derivation is based on a model for the electrode geometry shown in Figures A1 and A2. Interdigitated electrodes of length W, width L/2, and spaced L/2 apart (Figure A1) are modelled as a periodic array of alternating stripe electrodes (Figure A2). End and edge effects are ignored (a valid approximation since L = 0.025 cm and W = 0.76 cm). The total number of spaces between electrodes is N; thus, the total extent of the device in the x direction is NL. In our case, N = 84.

The expanded side view of Figure A2 illustrates the model used. The aluminum electrodes are represented as having zero thickness in the z direction. The glass substrate is represented as being semi-infinite. Each medium has a dielectric permittivity ε and a conductivity σ. In addition, the glass-polymer interface at $z = 0$ is assumed to have a surface conductivity κ_g, and the polymer-air interface is assumed to have a surface conductivity κ_p.

The structure is driven with a sinusoidal voltage of amplitude V applied between the positive and negative electrodes. Equivalently, the electrostatic potential $\phi(x,z,t)$ at $z = 0$ and $t = 0$ can be assumed to be the periodic function shown in Figure A3. The complete expression for $\phi(x,0,0)$, expressed as a Fourier series in x, is

$$\phi(x,0,0) = V \sum_{n_{odd}} \frac{8}{(n\pi)^2} \cos\frac{n\pi}{4} \cos\frac{n\pi x}{L} \cos \omega t \qquad \text{A.1}$$

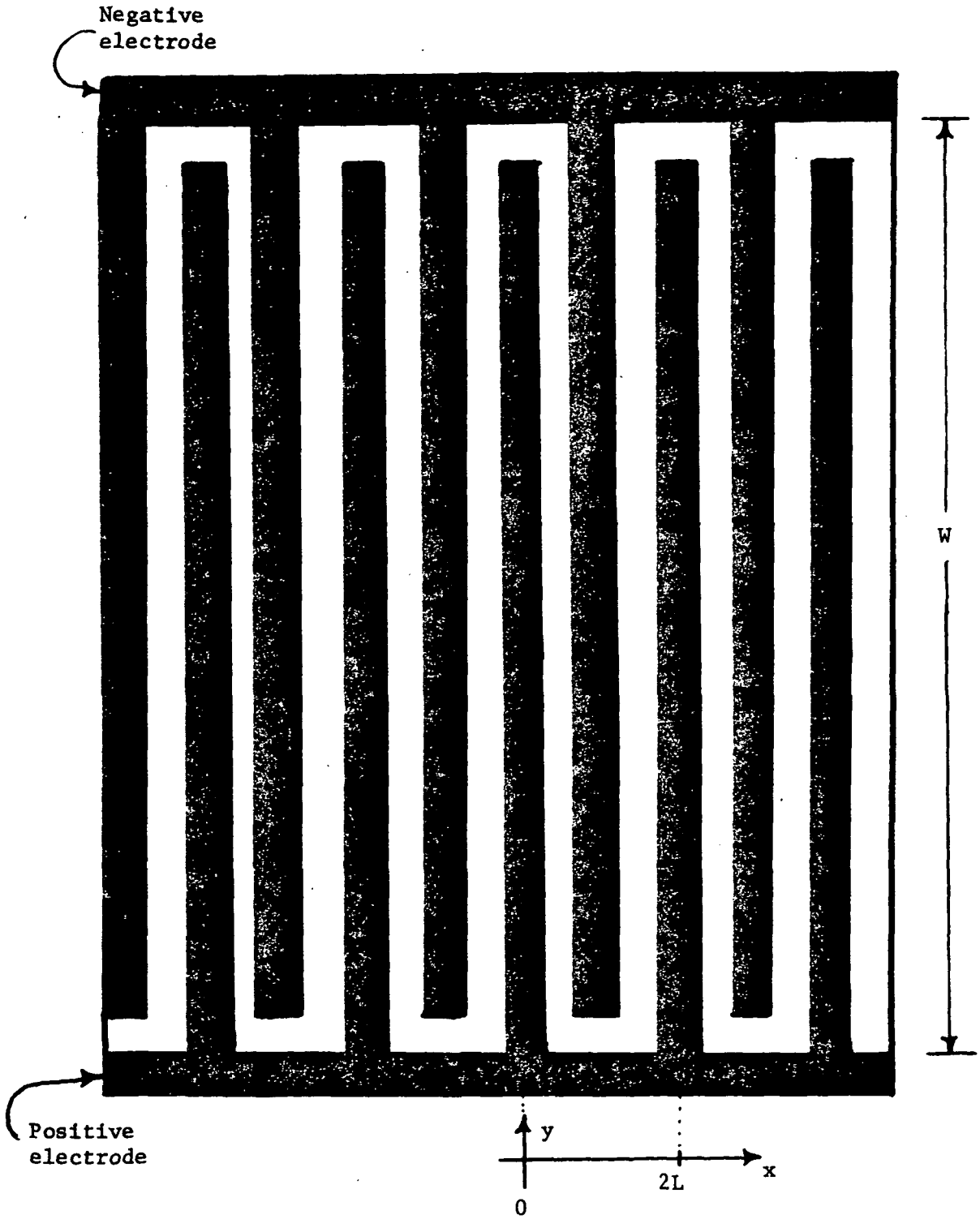

Figure A1: Schematic of top view of a portion of the lock-and-key device.

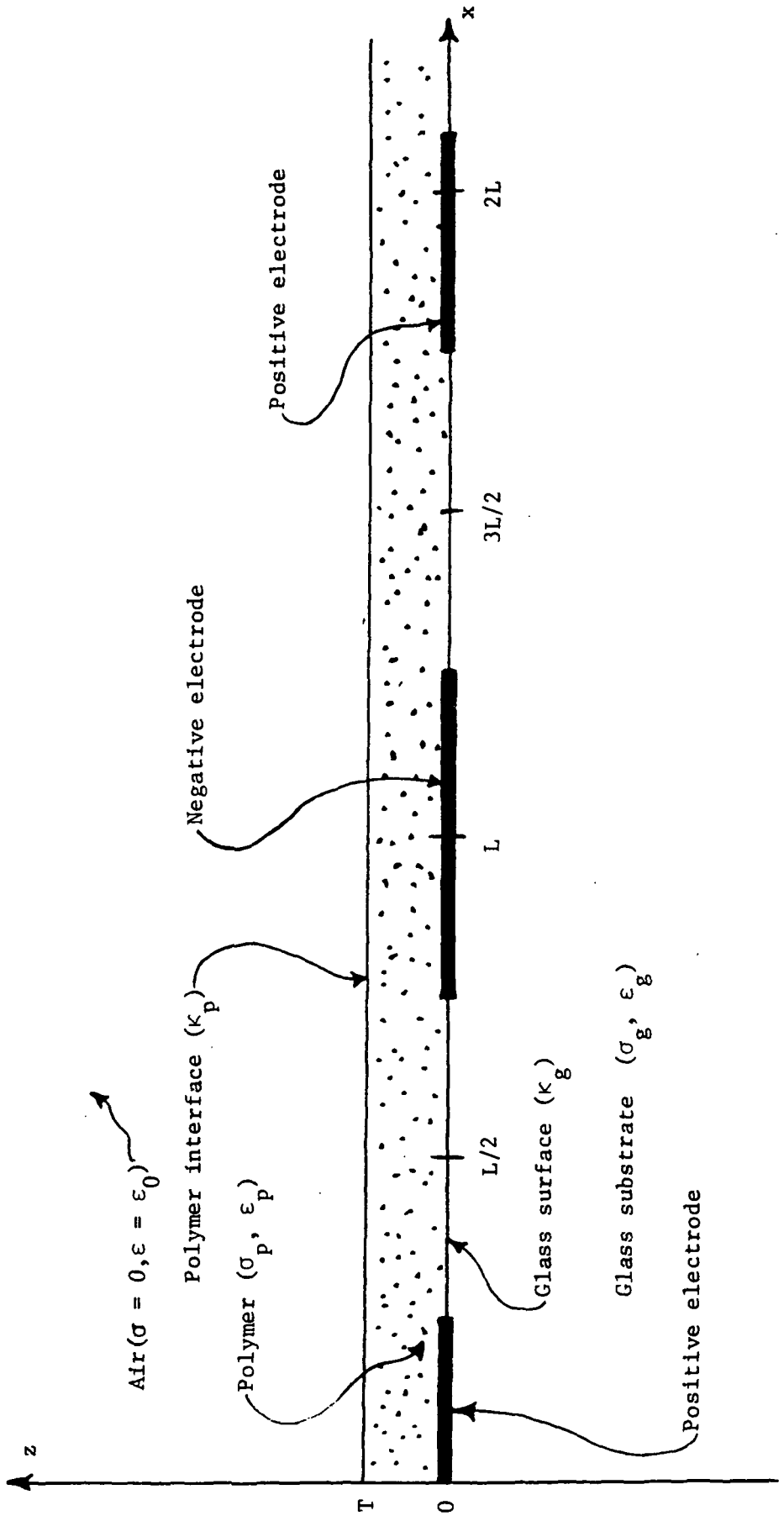

Figure A2: Expanded side view of a cross section of the lock-and-key device.

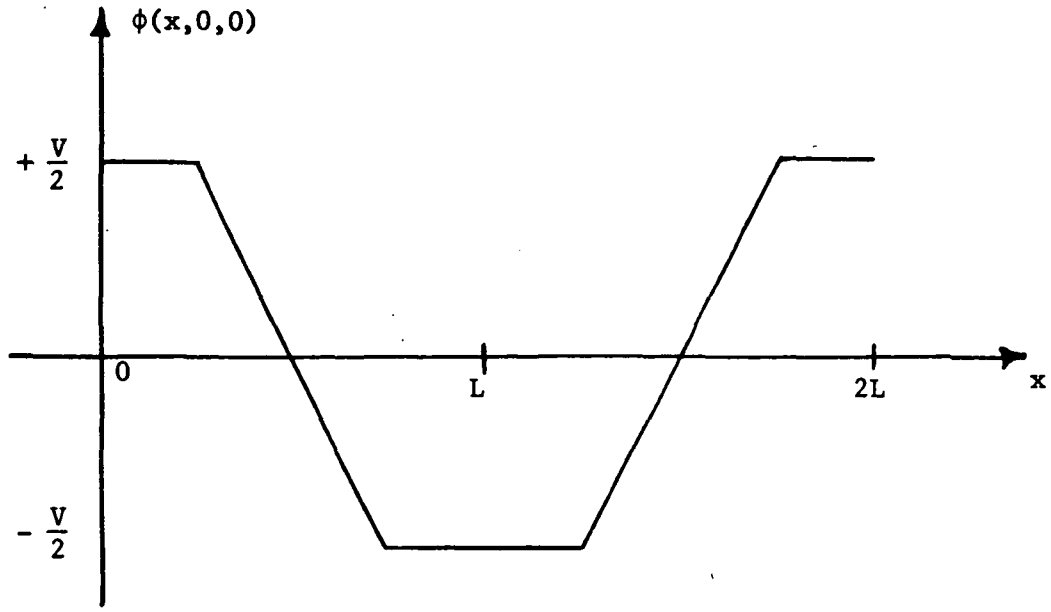

Figure A3: Periodic potential at z = 0, t = 0.

This potential function serves as a boundary condition for $\phi(x,z,t)$ throughout the structure. Because all media are linear, it is sufficient to find the response to a single sinusoid of the form

$$\phi(x,0,0) = \text{Re}\ \{A \cos kx\ e^{j\omega t}\} \qquad \text{A.2}$$

where for a typical term

$$k = \frac{n\pi}{L} \qquad \text{A.3}$$

$$A = \frac{8\,V}{n^2\pi^2} \cos\frac{n\pi}{4}$$

The potential is obtained by solving Laplace's equation for the potential subject to Eq. A.1 and to the following additional boundary conditions:

1) In the substrate, $\phi \to 0$ as $z \to -\infty$

2) At the polymer surface ($z = T$), the continuity equation requires that

$$\kappa_p \left.\frac{\partial^2\phi^I}{\partial x^2}\right|_{z=T} + j\omega\varepsilon_0 \left.\frac{\partial\phi^{II}}{\partial z}\right|_{z=T} - (\sigma_p + j\omega\varepsilon_p)\left.\frac{\partial\phi^I}{\partial z}\right|_{z=T} = 0 \qquad \text{A.4}$$

where ϕ^I is the potential function in the polymer and ϕ^{II} is the potential function in the air.

3) In the air, $\phi \to 0$ as $z \to +\infty$

The solution is

Region I: Polymer

$$\phi^I(x,z,t) = \text{Re}\left\{A \cos kx \left[\frac{\cosh k(T-z) + \alpha \sinh k(T-z)}{\cosh kT + \alpha \sinh kT}\right] e^{j\omega t}\right\} \qquad \text{A.5}$$

where

$$\alpha = \frac{k\,\kappa_p + j\omega\varepsilon_0}{\sigma_p + j\omega\varepsilon_p} \qquad \text{A.6}$$

Region II: In air

$$\phi^{II}(x,z,t) = \mathrm{Re}\left\{A \cos kx\left[\frac{e^{k(T-z)}}{\cosh kT + \alpha \sinh kT}\right] e^{j\omega t}\right\} \qquad \text{A.7}$$

Region III: In the substrate

$$\phi^{III}(x,z,t) = \mathrm{Re}\left\{A \cos kx\, e^{kz}\, e^{j\omega t}\right\} \qquad \text{A.8}$$

The admittance can be found from Eqs. A.5 - A.8 in several ways. The simplest way conceptually is to imagine a z-y plane at x = +L/2. The current density J_x crossing this plane is $-(\sigma + j\omega\varepsilon)\partial\phi/\partial x\big|_{x=L/2}$ for each of the three regions, and is $-\kappa_p\, \partial\phi^I/\partial x \,\big|_{x=L/2}\delta(z-T)$ at the polymer surface and $-\kappa_g\, \partial\phi^I/\partial x\big|_{x=L/2}\, \delta(z)$ at the glass surface. The total current is then

$$I = \mathrm{Re}\left\{2 \int_0^W dy \int_{-\infty}^{\infty} dz\, J_x\right\} \qquad \text{A.9}$$

where the factor of 2 accounts for the equal current crossing the plane at x = -L/2. Evaluating Eq. A.9, and multiplying by the number of identical cells (N/2) yields a complex admittance.

$$Y = NW \sum_{n_{odd}} (-1)^{\left(\frac{n-1}{2}\right)} \frac{8 \cos\frac{n\pi}{4}}{n^2\pi^2} \left\{(\sigma_p + j\omega\varepsilon_p)\left(\frac{\sinh\frac{n\pi T}{L} + \alpha_n \cosh\frac{n\pi T}{L}}{\cosh\frac{n\pi T}{L} + \alpha_n \sinh\frac{n\pi T}{L}}\right)\right.$$
$$\left. + (\sigma_g + j\omega\varepsilon_g) + \frac{n\pi\kappa_g}{L}\right\} \qquad \text{A.10}$$

where

$$\alpha_n = \frac{\frac{n\pi\kappa_p}{L} + j\omega\varepsilon_0}{\sigma_p + j\omega\varepsilon_p} \qquad \text{A.11}$$

The alternating signs lead to relatively rapid convergence of the Fourier series of Eqn. A.10, permitting the estimate

$$Y_{total} \tilde{\approx} 0.8\, Y_{first\ term} \qquad \text{A.12}$$

Making this approximation, and recognizing that $\pi T/L << 1$,

$$Y = 0.8 \frac{NW\ 4\ \sqrt{2}}{\pi^2} \{[\frac{\pi}{L}(\kappa_g + \kappa_p) + \sigma_g + \frac{\pi T}{L}\sigma_p] + j\omega[\varepsilon_0 + \varepsilon_g + \frac{\pi T}{L}\varepsilon_p]\} \qquad \text{A.13}$$

This admittance is equivalent to a conductance G in parallel with a capacitance C where

$$G = 0.8 \frac{NW\ 4\ \sqrt{2}}{\pi^2} \{\frac{\pi}{L}(\kappa_p + \kappa_g) + \sigma_g + \frac{\pi T}{L}\sigma_p\} \qquad \text{A.14}$$

$$C = 0.8 \frac{NW\ 4\ \sqrt{2}}{\pi^2} \{\varepsilon_0 + \varepsilon_g + \frac{\pi T}{L}\varepsilon_p\} \qquad \text{A.15}$$

These formulas constitute the basis for the interpretation of lock-and-key data.

APPENDIX B
CONTRACT PERSONNEL

A team of faculty, technical staff, and students was assembled to accomplish the contract tasks (see Table B-I). Senturia as principal investigator was responsible for overall project supervision; Fonstad contributed expertise on issues related to device fabrication, Colton on issues related to gas measurements. All persons listed in Table B-I participated on a part-time basis, sharing their time with other programs and committments (except during the summer of 1974, when Senturia and Hinson were effectively full time).

TABLE B-I

PERSONNEL

Principal Investigator:	Stephen D. Senturia Associate Professor of Electrical Engineering Co-Leader, Semiconductor Materials and Devices Group
Associate Investigators:	Clifton G. Fonstad Assistant Professor of Electrical Engineering
	Clark K. Colton Associate Professor of Chemical Engineering
Technical Support Staff:	Anthony Colozzi, Staff Engineer Jeffrey Kurtze, Staff Engineer Joseph Walsh, Project Technician Dorothy Chapman, Microelectronics David Hinson, Student Technician Barry Weichman, Student Technician